



# An evaluation of new parsimony-based versus parametric inference methods in biogeography: a case study using the globally distributed plant family Sapindaceae

Sven Buerki<sup>1,2\*</sup>, Félix Forest<sup>3</sup>, Nadir Alvarez<sup>4</sup>, Johan A. A. Nylander<sup>5</sup>, Nils Arrigo<sup>2</sup> and Isabel Sanmartín<sup>1\*</sup>

<sup>1</sup>Real Jardín Botánico – CSIC, Plaza de Murillo 2, 28014 Madrid, Spain, <sup>2</sup>Institute of Biology, University of Neuchâtel, Rue Emile-Argand 11, CH-2009 Neuchâtel, Switzerland, <sup>3</sup>Molecular Systematics Section, Jodrell Laboratory, Royal Botanic Gardens, Kew, Richmond, Surrey TW9 3DS, UK, <sup>4</sup>Department of Ecology and Evolution, Biophore, University of Lausanne, 1015 Lausanne, Switzerland, <sup>5</sup>Department of Botany, Stockholm University, SE-10691, Stockholm, Sweden

## ABSTRACT

**Aim** Recently developed parametric methods in historical biogeography allow researchers to integrate temporal and palaeogeographical information into the reconstruction of biogeographical scenarios, thus overcoming a known bias of parsimony-based approaches. Here, we compare a parametric method, dispersal–extinction–cladogenesis (DEC), against a parsimony-based method, dispersal–vicariance analysis (DIVA), which does not incorporate branch lengths but accounts for phylogenetic uncertainty through a Bayesian empirical approach (Bayes-DIVA). We analyse the benefits and limitations of each method using the cosmopolitan plant family Sapindaceae as a case study.

**Location** World-wide.

**Methods** Phylogenetic relationships were estimated by Bayesian inference on a large dataset representing generic diversity within Sapindaceae. Lineage divergence times were estimated by penalized likelihood over a sample of trees from the posterior distribution of the phylogeny to account for dating uncertainty in biogeographical reconstructions. We compared biogeographical scenarios between Bayes-DIVA and two different DEC models: one with no geological constraints and another that employed a stratified palaeogeographical model in which dispersal rates were scaled according to area connectivity across four time slices, reflecting the changing continental configuration over the last 110 million years.

**Results** Despite differences in the underlying biogeographical model, Bayes-DIVA and DEC inferred similar biogeographical scenarios. The main differences were: (1) in the timing of dispersal events – which in Bayes-DIVA sometimes conflicts with palaeogeographical information, and (2) in the lower frequency of terminal dispersal events inferred by DEC. Uncertainty in divergence time estimations influenced both the inference of ancestral ranges and the decisiveness with which an area can be assigned to a node.

**Main conclusions** By considering lineage divergence times, the DEC method gives more accurate reconstructions that are in agreement with palaeogeographical evidence. In contrast, Bayes-DIVA showed the highest decisiveness in unequivocally reconstructing ancestral ranges, probably reflecting its ability to integrate phylogenetic uncertainty. Care should be taken in defining the palaeogeographical model in DEC because of the possibility of overestimating the frequency of extinction events, or of inferring ancestral ranges that are outside the extant species ranges, owing to dispersal constraints enforced by the model. The wide-spanning spatial and temporal model proposed here could prove useful for testing large-scale biogeographical patterns in plants.

\*Correspondence: Sven Buerki, Molecular Systematics Section, Jodrell Laboratory, Royal Botanic Gardens, Kew, Richmond, Surrey TW9 3DS, UK and Isabel Sanmartín, Real Jardín Botánico – CSIC, Plaza de Murillo 2, 28014 Madrid, Spain. E-mail: s.buerki@kew.org and isanmartin@rjb.csic.es

**Keywords**

Bayesian analysis, biogeography, dispersal–extinction–cladogenesis, dispersal–vicariance analysis, divergence times, historical biogeography, palaeogeographical scenarios, parametric methods, Sapindaceae, speciation models.

**INTRODUCTION**

After a long period of ‘stagnation’ following the establishment of the vicariance paradigm and the rise to prominence of the cladistic biogeographical school in the mid to late 20th century (Croizat, 1952; Nelson & Platnick, 1981), the field of historical biogeography is going through an extraordinary revolution concerning its methods, underlying assumptions and the questions it aims to answer (Ree & Sanmartín, 2009). Cladistic biogeographical methods (also termed ‘pattern-based’; Ronquist, 1997) were designed to find patterns without making any assumptions about the underlying evolutionary processes (Ebach *et al.*, 2003; Parenti, 2006). The latter were inferred ‘*a posteriori*’ from the interpretation of results, making it difficult to compare alternative biogeographical scenarios statistically. ‘Event-based’ methods, such as dispersal–vicariance analysis (DIVA; Ronquist, 1997), represented an important step forwards in that they allowed the direct identification of events of interest to the biologist, such as dispersal, vicariance and extinction (Ronquist, 2003). However, as in cladistic methods, their reliance on the ‘principle of parsimony’ implied that sources of prior evidence other than the tree topology and the distribution of species, such as information on the times of divergence between lineages (Donoghue & Moore, 2003) or the connectivity of biogeographical areas through time (Sanmartín *et al.*, 2001), could not be directly incorporated into the biogeographical analysis (Sanmartín *et al.*, 2008).

In recent years a new class of parametric methods has been developed that is not constrained by the inherent biases of the parsimony approach (Ree & Sanmartín, 2009). Parametric methods model range evolution (i.e. the change in geographical range from ancestor to descendant) as a stochastic process with discrete states (geographical ranges) that evolve along the branches of the phylogeny according to a probabilistic Markov chain model. Transitions between states are assumed to occur stochastically according to an instantaneous rate matrix ( $Q$  matrix), whose parameters are biogeographical processes (i.e. extinction, range expansion, dispersal) determining the probability of range evolution – by contraction, range expansion or jump dispersal – from ancestor to descendant as a function of time. Relative to event-based and cladistic approaches, these methods offer the advantage that they allow the integration into biogeographical inference of estimates of the time of divergence between lineages. In addition, they can account for the uncertainty in ancestral range reconstruction because all possible biogeographical scenarios are evaluated by estimating the relative probabilities of ancestral areas. Finally, because the

underlying stochastic models are based on well-known probability distributions, parametric approaches provide a more rigorous statistical framework for the testing of alternative biogeographical hypotheses than event-based methods (Ree & Sanmartín, 2009; Sanmartín, 2010).

Recently, two new methods have been proposed that are based on explicit parametric models of biogeographical processes: a dispersal–extinction–cladogenesis (DEC) likelihood model (Ree *et al.*, 2005; Ree & Smith, 2008) and a Bayesian approach to island biogeography (Sanmartín *et al.*, 2008). The former is a parametric, extended version of dispersal–vicariance analysis that estimates by maximum likelihood ancestral ranges, transition rates between ranges and biogeographical scenarios of range inheritance for a group of taxa (Ree & Smith, 2008). One of the advantages of the DEC model is its flexibility: parameters in the transition matrix can be scaled or modified to reflect the changing palaeogeography, the availability of area connections (e.g. land bridges) through time or the dispersal capabilities of the study group of interest. One way to do this is by constraining the geographical ranges that are valid states in the model, thus reducing the size of the  $Q$  transition matrix. For example, one could exclude those ranges that span more unit areas than the current geographical range of extant species (Ree & Sanmartín, 2009). The DEC model has recently been used in several studies ranging from island scenarios (Clark *et al.*, 2008) to Holarctic biogeography (Smith, 2009) and Neotropical diversification (Santos *et al.*, 2009), while Sanmartín *et al.* (2010) recently applied the Bayesian island biogeographical method to reconstruct the origin of African disjunct floristic patterns (see Ree & Sanmartín, 2009, for more details on the latter method, especially in comparison with the DEC model).

Despite their potential advantages, model-based approaches are not without their own limitations. Primary among these is computational feasibility and how to balance this with inferential power and increasing realism of biogeographical scenarios. For methods allowing widespread states such as the DEC model, the size of the  $Q$  matrix increases exponentially with the number of areas in the analysis. Therefore, careful area definition becomes very important with regard to the type of question and considering alternative sources of information such as palaeogeographical scenarios or species ecological tolerance (Ree & Sanmartín, 2009).

In comparison with parametric approaches, an event-based method such as dispersal–vicariance analysis (DIVA) offers the advantage that it does not require any prior knowledge of the geological history of the areas studied (i.e. the timing of

geographical barriers and connection routes) or lineage divergence times (Nylander *et al.*, 2008a), and can therefore be applied to phylogenies where branch lengths are meaningless or difficult to interpret (e.g. morphology-based cladograms). Recent comparisons between DIVA and its parametric counterpart, the DEC model, show that for some biogeographical scenarios the two methods provide similar solutions (e.g. Ree *et al.*, 2005; Xiang & Thomas, 2008). Probably the biggest limitation of DIVA, more than the optimization algorithm itself, is the fact that ancestral areas must be reconstructed onto a fixed and fully resolved topology. This is problematic, because polytomies and weak nodal support are common features in many phylogenies due to low phylogenetic signal. To address this problem, Nylander *et al.* (2008a) proposed an empirical Bayesian approach to dispersal–vicariance analysis (Bayes-DIVA) that integrates DIVA biogeographical reconstructions over the posterior distribution of the tree topology from a Bayesian Markov chain Monte Carlo (MCMC) analysis. This approach allows an estimation of marginal probabilities of ancestral ranges for a given node while integrating over the uncertainty in the rest of the tree topology. Further, accounting for the uncertainty in phylogenetic relationships may sometimes reduce the uncertainty in the biogeographical reconstruction itself (Nylander *et al.*, 2008a). To date, Bayes-DIVA has been used in several empirical plant studies dealing with regional scenarios (e.g. Antonelli *et al.*, 2009; Roquet *et al.*, 2009; Espíndola *et al.*, 2010).

In a recent comparative study in ancestral range reconstruction methods, Clark *et al.* (2008) compared parametric versus parsimony-based approaches with biogeographical inference in the context of island biogeographical scenarios. They found that methods that incorporate branch lengths and/or timing of events, such as the DEC model, gave more plausible area range histories. They encouraged the use of other biogeographical systems, such as continental lineages, to further illustrate the comparative performance of the methods.

In this study, we compare the parsimony-based Bayes-DIVA method against a fully parametric method, the DEC likelihood model (Ree & Smith, 2008). Both methods model dispersal (geographical movement) as the result of allopatric speciation following range expansion and are thus appropriate for the analysis of continental biogeographical scenarios in which areas are spatially contiguous and there is no jumping over oceanic barriers. The benefits and limitations of these methods are compared using the cosmopolitan plant family Sapindaceae as a case study. The distribution of this family spans all continents and its fossil record indicates that its biogeographical history traces back to the Early Cretaceous (see below). Previous implementations of the DEC model have been limited to small studies in terms of spatial (Clark *et al.*, 2008), temporal (Santos *et al.*, 2009) or taxonomic (Smith, 2009) scales. Here, we propose a complex biogeographical model that reflects changes in continental configurations during the last 110 million years and spans all continents.

## MATERIALS AND METHODS

### The study group

Several lines of evidence support the choice of Sapindaceae as an ideal case study for investigating the performance of biogeographical methods. Recent phylogenetic studies have supported the monophyly of this mid-sized (*c.* 140 genera, *c.* 1900 species) cosmopolitan family (Buerki *et al.*, 2009). Based on molecular and morphological characters, Buerki *et al.* (2009) subdivided Sapindaceae into four subfamilies: Xanthoceroideae, Hippocastanoideae, Dodonaeoideae and Sapindoideae. The first two subfamilies occur in temperate regions, whereas the two remaining are widely distributed in the tropical regions. Sapindaceae genera range from narrow endemics (e.g. the newly described genus *Gereaua* in Madagascar; Buerki *et al.*, 2010a), to those occurring on two continents (e.g. *Cupaniopsis*, found in Australia and southern Asia), to those widespread across the tropics (e.g. *Allophylus*). In addition, several fossils associated with monophyletic genera provide reliable calibration points for divergence time estimations.

### Dataset

The dataset used to estimate lineage divergence times and ancestral ranges in Sapindaceae is based on that of Buerki *et al.* (2009), with the addition of several taxa required to calibrate the divergence time analyses (e.g. *Allophylus*, *Paullinia*; see Buerki *et al.*, 2010b). Ingroup sampling comprised 148 accessions representing > 60% of the generic diversity and two outgroup taxa: *Sorindeia* sp. (Anacardiaceae; used as the most external outgroup) and *Harrisonia abyssinica* (Simaroubaceae). Species names, voucher information and GenBank accession numbers for all sequences are provided in Buerki *et al.* (2010b). The DNA extraction, amplification and sequencing protocols for one nuclear ribosomal region (internal transcribed spacer region, ITS) and seven plastid regions (coding *matK* and *rpoB*, non-coding *trnL* intron and the inter-genic spacers *trnD–trnT*, *trnK–matK*, *trnL–trnF* and *trnS–trnG*) are provided in Buerki *et al.* (2009).

### Phylogenetic analyses

Bayesian MCMC was used to approximate the posterior probability distribution of the phylogeny based on the combined plastid–nuclear dataset, using MrBayes v.3.1.2 (Ronquist & Huelsenbeck, 2003). To decrease the complexity and increase mixing in the MCMC, the dataset was divided into two partitions, nuclear (including only the ITS region) and plastid (including the seven plastid markers), and each locus was allowed to have partition-specific model parameters (Ronquist & Huelsenbeck, 2003; Nylander *et al.*, 2004). Buerki *et al.* (2009) had previously shown that there was no incongruence between the nuclear and plastid datasets. Model selection for the data partitions in the MCMC was carried out

with MrMODELTEST2 v.2.3 (Nylander, 2004). For both partitions, the best-fitting model was the general time reversible (GTR) model with an alpha parameter for the shape of the gamma distribution to account for rate heterogeneity among sites. Three Metropolis-coupled Markov chains with an incremental heating temperature of 0.2 were run for 50 million generations and sampled every 1000th generation. The analysis was repeated twice, starting from random trees. Convergence of the MCMC was verified using the effective sample size criterion for each parameter as implemented in TRACER v.1.4 (Rambaut & Drummond, 2007) and by monitoring cumulative posterior split probabilities and among-run variability of split frequencies using the online tool AWTY (Nylander *et al.*, 2008b). Because of the high number of trees and to avoid misleading relationships caused by underestimated burn-in, 80% and 85% of the trees, respectively, from run one and two were discarded and the remaining samples from the independent runs were combined to obtain a final approximation of the posterior probability distribution of the phylogeny (based on 15,362 trees in total).

The posterior distribution of trees was summarized using the allcompat consensus from MrBAYES (50% consensus majority rule with compatible groups added) instead of the commonly used 50% halfcompat consensus. The reason for this was to obtain a completely resolved topology – a requirement of the LAGRANGE analysis (see below) – and to simplify detailed comparisons of all nodes between the Bayes-DIVA and LAGRANGE analyses. Nonetheless, with the exception of two polytomies affecting terminal nodes, the allcompat and halfcompat consensus were identical.

### Estimation of lineage divergence times

A likelihood ratio test (Felsenstein, 1988) was used to determine whether sequence data conformed to the expectation of a molecular clock following the same procedure as Forest *et al.* (2007) and using a maximum likelihood total evidence tree produced with RAxML v7.0.0 (Stamatakis, 2006) as in Buerki *et al.* (2009). The likelihood ratio test strongly rejected the molecular clock:  $D = 2 [69029.95–68302.98] = 726.97$ , 148 d.f.,  $P < 0.001$ .

Given the lack of a molecular clock, relative branching times were estimated on the allcompat consensus using penalized likelihood (PL; Sanderson, 2002), as implemented in r8s v.1.71 (Sanderson, 2004), and the truncated Newton method algorithm. The smoothing value (320) was established using the cross-validation routines implemented in r8s. The most external outgroup, *Sorindeia* sp. (Anacardiaceae), was pruned for the estimation of the divergence time as required by the program (see Sanderson, 2004).

To account for phylogenetic uncertainty in the estimation of lineage divergence times and to investigate its effect on biogeographical reconstructions (see below), we performed PL analyses on a random sample of trees ( $n = 1000$ ) from the Bayesian MCMC stationary distribution, after discarding those trees that did not conform with the calibration constraints, i.e.

trees that did not support the monophyly of clades to which a fossil calibration point was attached (see below). In all, we discarded 236 trees, < 2% of all trees. The same smoothing parameter value was used on all sampled trees. TREEANNOTATOR v.1.4.7 (Drummond & Rambaut, 2007) was used to estimate mean values and 95% confidence intervals of age estimates from the sample of 1000 PL-dated trees for each node in the allcompat consensus tree. In addition, we used R scripts (R Development Core Team, 2009; available from S.B. on request) to extract minimum, median and maximum nodal age estimates from the sample of PL-dated trees and to plot these onto the allcompat consensus tree. Alternatively, we tried to use a Bayesian relaxed clock approach (BEAST; Drummond & Rambaut, 2007) to estimate the posterior probability distribution of nodal heights but failed to reach convergence after several attempts, probably due to the size and complexity of the dataset, i.e. 150 taxa and eight different DNA markers.

### Fossil calibration

To estimate absolute ages for lineage divergences we used six fossil calibration points (see below) within Sapindaceae to set minimum age constraints for several nodes in the phylogeny. For each calibration point, the oldest fossil record was selected and the upper (younger) bound of the geological interval (Gradstein & Ogg, 2004) in which the fossil was found was used to represent the minimum age constraint.

Calibration points were defined as follows: (1) the root node, i.e. the most recent common ancestor of Sapindaceae and Simaroubaceae, was constrained to a maximum age of 125 Ma; (2) the stem group of *Acer*, *Aesculus* and *Dipteronia* was constrained to a minimum age of 55.8 Ma; (3) the stem group of *Dodonaea* and *Diplopeltis* was constrained to a minimum age of 37.2 Ma; (4) the stem group of *Koelreuteria* was constrained to a minimum age of 37.2 Ma; (5) the stem group of *Pometia* was constrained to a minimum age of 5.33 Ma; and (6) the stem group of *Cardiospermum*, *Paullinia* and *Serjania* was constrained to a minimum age of 37.2 Ma. Fossil evidence supporting each calibration point (and associated references) is listed in Appendix S1 in Supporting Information.

### Biogeographical analyses

#### Areas

In plants, the definition of areas for biogeographical analysis, especially at a world-wide scale, remains controversial (e.g. Cox, 2001). Most researchers circumscribe areas according to the ecological tolerance and current distribution patterns of their group of interest ('criterion of sympatry'). This has the problem that different groups may exhibit different distribution patterns and therefore area definition may not be comparable across groups. In this study we used a geological criterion similar to that of Sanmartín & Ronquist (2004), and defined areas of study according to palaeogeographical history

(i.e. plate tectonics). This approach has the advantage of decreasing the subjectivity in area definition and can be applied to different plant groups when focusing on large-scale biogeographical patterns.

To minimize the effect of taxon sampling bias in our analysis, generic distributions were assigned to terminal branches (following Buerki *et al.*, 2009), except when the genus was recognized as para- or polyphyletic (e.g. *Cupaniopsis*; see Buerki *et al.*, 2009, for more details), in which case terminals were scored according to the distribution of the species.

In all, seven geographical areas were defined (Fig. 1): A, Eurasia, from western Europe to Indochina; B, Africa; C, Madagascar, including the Comoro Islands and the Mascarene Islands; D, Southeast Asia, including India, the Malaysian Peninsula, the Philippines, Sumatra, Borneo and the Inner Banda Arc, as well as the Pacific Islands (e.g. Hawaii); E, Australia, including New Guinea, New Caledonia and New Zealand; F, North America; G, South America, including Central America and the West Indies.

Area D (Southeast Asia) has a complex palaeogeographical (and biogeographical) history, involving numerous small terranes that rifted away from Gondwana during the Palaeozoic–Mesozoic and were progressively accreted to the southern part of the Eurasian Plate (north China) at different times during the Mesozoic and Cenozoic (Metcalfe, 1998). South China and Indochina were the first to be accreted in the Late Devonian–Early Carboniferous, followed by the Quiantang and Sibumasu blocks (the eastern half of the Malaysian Peninsula) in the Permian–Triassic, whereas south-western Borneo and the Semitau terranes were derived from the

margin of Cathaysia land (south China and Indochina) by the opening of a marginal basin in the Cretaceous–Tertiary (Metcalfe, 1998). The remaining insular Southeast Asian terranes (Sumatra, the rest of Borneo, Celebes, the Inner Banda Arc, etc.) were formed as a result of the collision of the Australian Plate with the Eurasian Plate during the Cenozoic. This composite palaeogeographical history has two consequences in our biogeographical model. Firstly, area A (Eurasia) is here defined as including South China and the entire Indochina Peninsula (Fig. 1), because these terranes were already accreted to the Eurasian Plate by the time of the estimated origin of Sapindaceae in the Early Cretaceous (see Sanmartín *et al.*, 2001). Secondly, area D did not exist as we know it today until the Cenozoic (thus, it was not present at the time of origin of Sapindaceae), so we need to distinguish between a ‘proto-Southeast Asia’, the older parts of the Malaysian Peninsula and south-western Borneo, which were already in place by the Cretaceous–Tertiary boundary, and insular Southeast Asia, which did not appear until the Middle–Late Cenozoic. As seen below, this changing configuration of area D plays a very important role in the definition of our biogeographical model.

#### Biogeographical inference

*Bayes-DIVA*. Dispersal–vicariance analysis (DIVA) is a parsimony-based method that optimizes ancestral areas onto the nodes of phylogeny by minimizing the number of dispersal and extinction events (Ronquist, 1997). Area relationships are not constrained to follow a hierarchical pattern, so the method can be used to reconstruct reticulate biogeographical

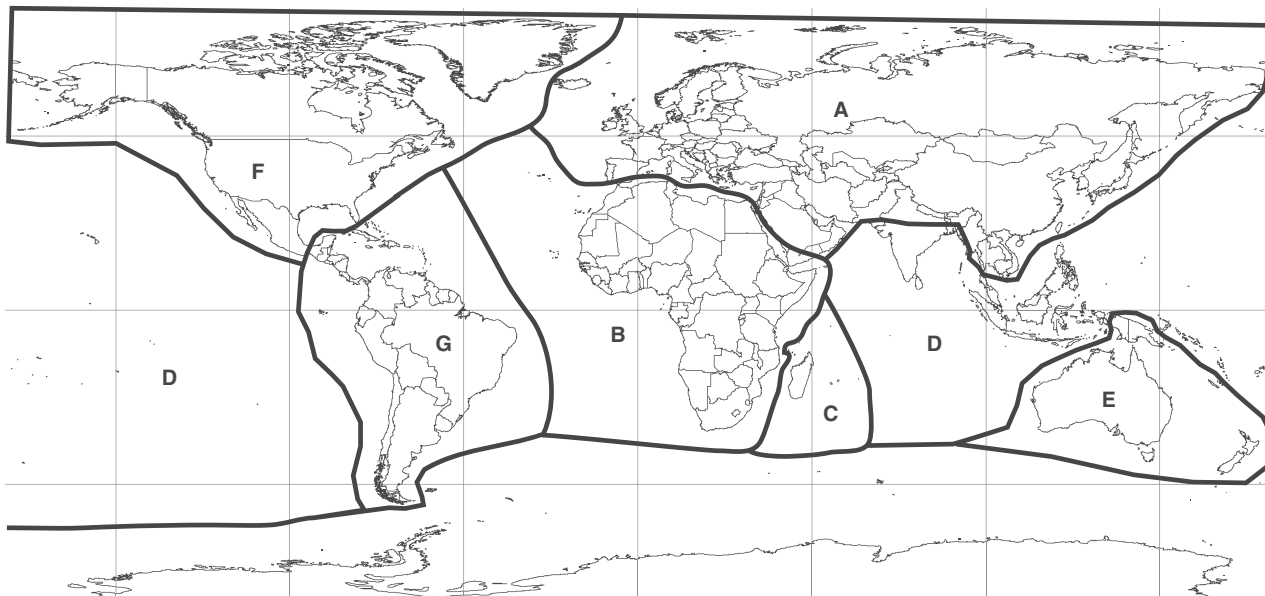


**Figure 1** Biogeographical regions used in the study of Sapindaceae. Key: A, Eurasia: from western Europe to Indochina; B, Africa; C, Madagascar, including the Comoro Islands and the Mascarene Islands; D, Southeast Asia, including India, the Malaysian Peninsula, Philippines, Sumatra, Borneo and the Inner Banda Arc, as well as the Pacific Islands (e.g. Hawaii); E, Australia, including New Guinea, New Caledonia and New Zealand; F, North America; G, South America including Central America and the West Indies.

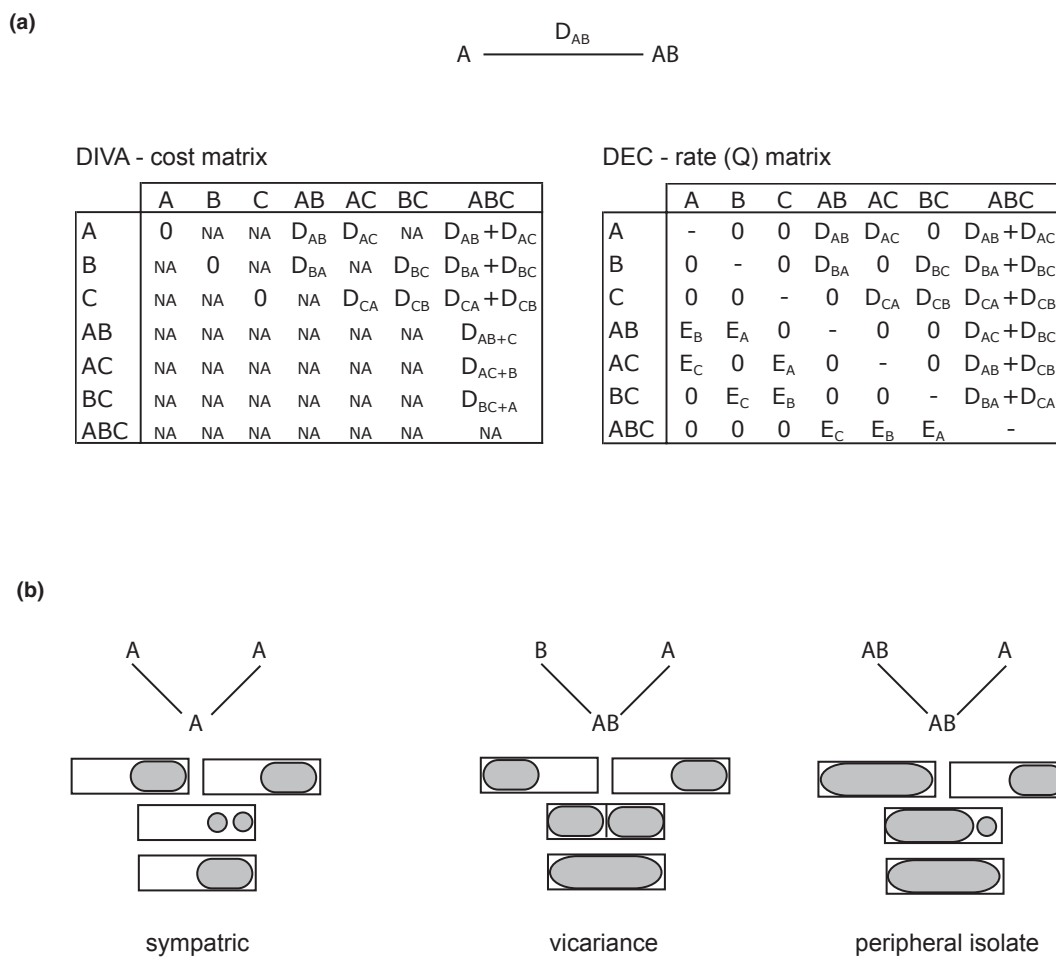


**Figure 2** Biogeographical models used by parsimony-based dispersal–vicariance analysis (DIVA) and its parametric counterpart, the dispersal–extinction–cladogenesis (DEC) model. There are two components in the model. (a) Anagenetic (internode) evolution. Left: DIVA uses a three-dimensional transition cost matrix to estimate the cost of change in geographical range between the ancestor and the left and right descendants. There are two events that can change the geographical range of the ancestor: dispersal is the addition of one or more unit areas to the ancestral range and with a cost = 1 per area added (e.g. AB to ABC =  $D_{AB+C} = 1$ ; A to ABC =  $D_{AB} + D_{AC} = 2$ ). Extinction is the deletion of one or more unit areas (cost = 1), but it is actually never inferred in the optimization unless explicit geographical constraints are used in the model (see text). Notice that if there is no change in geographical range, the cost is zero (e.g. A to A = 0), but that inheritance of widespread ancestral ranges is not allowed in DIVA (e.g. from AB to AB = NA). Right: In the DEC model, range evolution along a phylogenetic branch is governed by a matrix of instantaneous transition rates (Q matrix) whose parameters are dispersal (range expansion, e.g.  $D_{AB}$ ) and local extinction (range contraction,  $E_A$ ). Note that only rates separated by a single dispersal or extinction event are allowed in the matrix; all other transitions have an instantaneous rate of zero (e.g. A to B = 0). For transitions involving dispersal, the rate is the sum of rates from areas in the starting range  $d$  to the area of expansion  $d'$  (AB to ABC =  $D_{AC} + D_{BC} = 2d$ ). (b) Cladogenetic range evolution: inheritance of geographical ranges at nodes follows three different modes of speciation: sympatric speciation, for single-area ancestors, and allopatric speciation (vicariance) and/or peripheral-isolate speciation for widespread ancestors. DIVA only allows the first two speciation modes, while LAGRANGE implements all three of them. Notice that both methods model dispersal as range expansion leading to a widespread ancestor, followed by range division (e.g. ‘vicariance-mediated speciation’). D, dispersal or range expansion between areas; E, local extinction within an area; NA, not applicable. See text for more details on the methods.

scenarios with changing continental configurations (Ronquist, 1997; Sanmartín, 2007). DIVA uses a three-dimensional cost matrix to estimate the cost of moving from the ancestor to each of the left and right descendants (see Fig. 2a). There are two events that occur along internodes connecting two speciation events. Dispersal is the addition of one or more unit areas to the ancestral distribution and costs 1 per area added. It is equivalent to range expansion and it is always

followed by vicariance (Ronquist, 1997). Extinction is the deletion of one or more unit areas from the ancestral distribution and costs 1 per area deleted, but extinction events are actually never inferred by DIVA unless explicit geographical constraints are placed onto the model by changing the original cost matrix (Ronquist, 1996; Nylander *et al.*, 2008a). DIVA allows two different range inheritance scenarios at speciation nodes (Fig. 2b): (1) duplication or within-area

(‘sympatric’) speciation when the ancestor is distributed in a single area and the two descendants each inherit the entire ancestral range (A to A, Fig. 2b); and (2) vicariance when the ancestor occurs in two or more areas and each descendant inherits a non-overlapping subset of the ancestral range (AB to A and B, Fig. 2b). The cost of these two events is zero. Notice that inheritance of widespread ancestral ranges (e.g. AB to AB in Fig. 2a) is not allowed in DIVA: ancestral widespread distributions are always divided by vicariance at speciation nodes (Sanmartín, 2007). Ancestral ranges at nodes are optimized by minimizing the dispersal (extinction) cost associated with moving from the ancestral range to the two descendant (left and right) ranges.

Uncertainty in phylogenetic relationships was accounted for in DIVA by using the Bayes-DIVA approach of Nylander *et al.* (2008a). Specifically, we ran DIVA analyses over the post-burn-in sample of the Bayesian MCMC analysis (15,362 in total) and used Nylander *et al.* (2008a) scripts to summarize/average ancestral area reconstructions over all sampled trees for each node in a reference tree, in this case the allcompat tree.

Two Bayes-DIVA analyses were run: (1) with no constraint in the maximum number of areas allowed at ancestral nodes, and (2) with the maximum number of areas constrained to two. Except for higher uncertainty in the assignment of ancestral ranges (i.e. lower marginal probabilities), results from the unconstrained Bayes-DIVA analysis were highly congruent with the more restricted analysis, with the largest differences found at the deeper nodes. As it is highly improbable that the ancestor of Sapindaceae was widespread over all continents – most species of Sapindaceae are restricted to one or two areas – only results from the maximum range size of two-areas analysis are shown here.

**DEC.** In the DEC model – implemented in the software LAGRANGE v. 2.0.1 (Ree & Smith, 2008) – range evolution along phylogenetic branches (internodes) is governed by a Q matrix of instantaneous transition rates (Fig. 2a), whose parameters are dispersal and local extinction describing the rate of geographical change from ancestor to descendant by range expansion and range contraction, respectively (Ree & Smith, 2008). The DEC model assumes that only one event, a single dispersal or local extinction event, can occur in an instant of time (Ree & Sanmartín, 2009). Therefore, those transitions that imply more than one event are given a rate of 0 in the Q matrix (Fig. 2a). For example, moving from A to B would imply a range expansion event from A to B ( $D_{AB}$ ) followed by an extinction event in A ( $E_A$ ), so this transition is given an instantaneous rate of zero in the matrix (Fig. 2a).

Cladogenetic evolution at speciation nodes is modelled as three alternative range inheritance scenarios (Ree *et al.*, 2005). For ancestors present in a single area, the two descendants form within and inherit the entire ancestral area (sympatric speciation as in DIVA; Fig. 2b). For widespread ancestors, lineage divergence could arise either between a single area and the rest of the range (vicariance or allopatric speciation as in DIVA) or within a single area – ‘peripheral isolate speciation’ (Ree & Smith, 2008) – in which case one descendant inherits a

range of just the area where the divergence occurred, while the other descendant inherits the entire ancestral range (Fig. 2b; Ree *et al.*, 2005). Such scenarios lead to non-identical range inheritance. Thus, unlike DIVA, the DEC model allows inheritance of widespread ancestral ranges at speciation nodes but only for one of the descendants (AB to A and AB, Fig. 2a). In other words, as in DIVA, a widespread ancestral range cannot be inherited in its entirety by the two descendants: AB to AB and AB (Ree *et al.*, 2005). Using standard maximum likelihood algorithms, the DEC method first estimates global rates of dispersal and extinction by integrating over all possible ancestral states at internal nodes in the phylogeny, and uses these rates to estimate node-by-node relative probabilities for ancestral areas and range inheritance scenarios without conditioning on any other range inheritance scenario in the rest of the tree (Ree & Smith, 2008).

Like Bayes-DIVA, LAGRANGE analyses were first run unconstrained (M0, all combinations of the seven areas allowed) and then constrained to include only ancestral ranges that span a maximum of two areas (M1). The LAGRANGE M0 analysis provided very similar results to the LAGRANGE M1 analysis, but with higher levels of biogeographical uncertainty (i.e. lower probability values; data not shown). It also required at least five times more computational power than the constrained M1 model. Therefore, in order to provide comparable results with the Bayes-DIVA analysis, only results from the constrained LAGRANGE M1 analyses are provided here. One drawback of the DEC analysis is that, unlike DIVA, where the maximum number of areas at ancestral nodes can be constrained independently from the distribution of the terminals, the Q transition matrix in LAGRANGE required the inclusion of a few ancestral ranges covering three, four and five unit areas, which were present in the most widespread terminals (e.g. *Dodonaea viscosa* in ABCDEG). This is because maximum likelihood inference of ancestral ranges at nodes is conditional on the range distribution of the descendants (Ree *et al.*, 2005), so all widespread terminal ranges must be allowed in the Q matrix for LAGRANGE analyses to converge.

**Stratified biogeographical model** (Fig. 3 and Appendix S1). In order to account for the changing palaeogeography over which Sapindaceae evolved, and to take advantage of the flexibility of the DEC model, we performed a new LAGRANGE analysis (here termed LAGRANGE Str) in which we stratified the phylogeny into different time slices reflecting the changing continental configuration over time, as tectonic plates broke up, moved apart or collided with each other through time. When constructing a stratified biogeographical model, care should be taken not to divide it too finely so that there are enough phylogenetic events in each time slice (Ree & Sanmartín, 2009). Here we chose to divide our model into four time slices (TS) that reflect the main palaeogeographical changes during the history of Sapindaceae: before 80 Ma, between 80 and 65 Ma, between 65 and 30 Ma, and between 30 Ma and the present day (Fig. 3). For each time slice, we defined a Q matrix in which transition rates were made dependent on the geographical connectivity between areas (i.e. through land

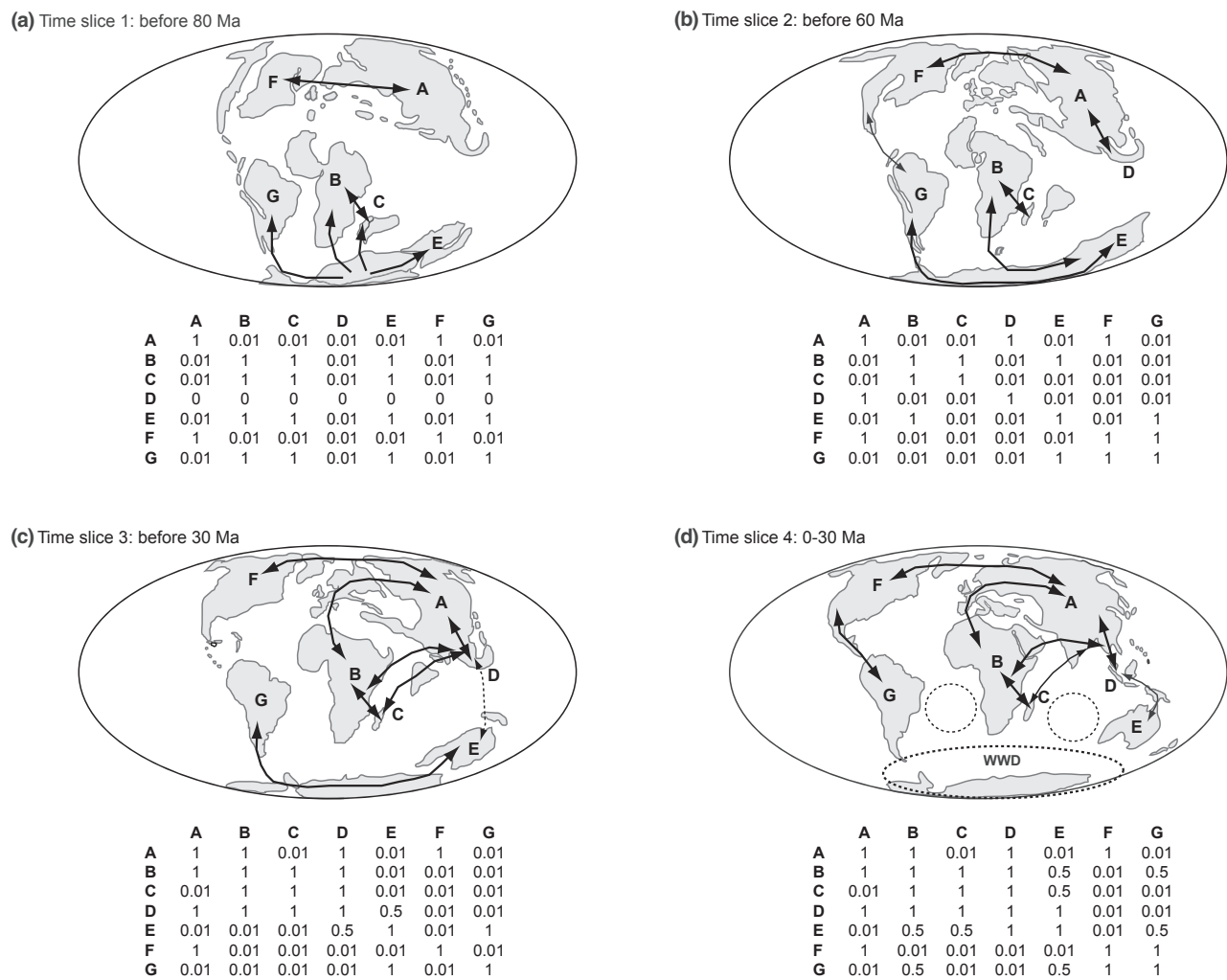


**Figure 3** Palaeogeographical model used in the Sapindaceae analysis, with four time slices reflecting the probability of area connectivity through time. Key: bold and dashed arrows represent, respectively, dispersal probabilities of 1 and 0.5; dashed circles symbolize the subequatorial current and the West Wind Drift (WWD) with a dispersal probability of 0.5. See Fig. 1 for details on coding and circumscription of areas.

bridges, changing sea levels, wind currents, etc.). This was done by scaling the rate of dispersal in the Q matrix according to the availability of area connections through time. For example, the dispersal rate between two areas that were not tectonically connected at a given time slice was downweighted by a factor of 0.01 to reflect the low probability of movement between those two areas, e.g. dispersal between South America and Africa was disallowed in the model after the final opening of the South Atlantic Ocean c. Ma (Fig. 3b). Dispersal through abiotic factors such as wind or ocean currents was scaled down to 0.5 of the global dispersal rate, as it usually involves a more restrictive, stochastic ‘sweepstakes’ dispersal, e.g. movement among the southern continents was partially allowed from the Early Oligocene onwards (Fig. 3d) after the establishment of the Equatorial and West Wind Drift currents. In contrast, dispersal between Eurasia and North America was allowed across all four time slices, via either the North Atlantic or the Beringian Strait (see Appendix S1 for a more detailed

description of our time-sliced palaeogeographical model and its translation into dispersal-scaling matrices in the LAGRANGE Str analysis).

A preliminary analysis showed considerable uncertainty in the root node ancestral area and all subsequent basal nodes, especially the most recent common ancestor of Dodonaeoideae (results not shown). As mentioned above, maximum likelihood inference of geographical ranges at ancestral nodes in LAGRANGE is conditional on the range distribution of the terminals (Ree *et al.*, 2005). This had the effect in our analysis of increasing the uncertainty at deeper nodes in the tree, as widespread terminal ranges are dragged back towards the root in the upward inference pass. This is the case for the Dodonaeoideae clade, which includes numerous widespread genera (e.g. *Dodonaea*, *Filicum* and *Ganophyllum*) and is also subtended by a relatively long branch, increasing the uncertainty in the inferred ancestral range. Because area A was inferred as the ancestral area with the highest probability for

the root node in both Bayes-DIVA and LAGRANGE M1 (see below), we constrained the ancestral range of the root node in the LAGRANGE Str analysis to area A in order to decrease the uncertainty in the rest of the basal nodes. Actually area A also received the highest likelihood in the LAGRANGE Str analysis in which the root nodal range was not constrained (albeit not significantly). Nonetheless, to avoid any bias in comparing the different methods, results from the root node reconstruction are not discussed below.

### Integrating biogeographical and dating uncertainty

To assess the impact of uncertainty in divergence time estimations in biogeographical reconstructions, we ran LAGRANGE analyses (M1 and Str) over three chronograms representing the ‘minimum’ (Min PL), ‘median’ (Med PL) and ‘maximum’ (Max PL) values of nodal ages as estimated over a sample of 1000 PL-dated trees. We then recorded the ancestral ranges inferred for each node on the allcompat consensus for comparison. We were especially interested in those nodes for which the interval between minimum and maximum node age spread across two different time slices.

To assess the congruence between biogeographical scenarios inferred by Bayes-DIVA and LAGRANGE, we first recorded the ancestral range that received the highest relative probability for each node in the allcompat consensus tree and compared these ranges pairwise between the three methods: Bayes-DIVA, LAGRANGE M1 and LAGRANGE Str. We considered two types of incongruence: (1) ‘hard area incongruence’, different methods inferred different ancestral range/s with the maximum relative probability; and (2) ‘soft area incongruence’, different methods inferred the same ancestral range/s but with different maximum relative probabilities. Second, for each method we estimated the mean maximum probability assigned to ancestral ranges across all nodes in the allcompat consensus, and compared these means statistically by using a Wilcoxon rank test. This provided a first evaluation of the level of biogeographical confidence or ‘decisiveness’ in area assignment for each method: the higher the mean value of the maximum probability assigned to ancestral ranges across the tree, the higher the level of decisiveness of the method and the lower its level of uncertainty in the inference of ancestral ranges. Third, we plotted the ancestral ranges inferred by each of the three methods onto the Median PL chronogram and compared these figures pairwise to identify differences in biogeographical scenarios. Using R scripts (available from S.B. on request), we recorded for each node in the phylogeny the area with the highest relative probability, the node age and – only for LAGRANGE – the length of the branch separating this node from its descendant. We used these data together with the matrix describing the cost or rate of moving between geographical states (Fig. 2) to build dispersal/extinction contingency tables showing the type and frequency of transition events (i.e. changes in geographical range) between ancestral and descendant nodes in the phylogeny. These contingency tables were then used to estimate the frequency and direction

of dispersal events in Bayes-DIVA and LAGRANGE, and the frequency of extinction events in LAGRANGE. Notice that there are two types of extinction events in LAGRANGE models: ‘observed’ extinction events in which an ancestral range is reduced by range contraction (e.g. AB to A in Fig. 2a), and ‘predicted’ extinction events that are required by the model, for example direct dispersal from A to G requires a range expansion ( $D_{AG}$ ) followed by an extinction in A ( $E_A$ ) (see Tables S1–S3 in Appendix S2). Finally, the number of dispersal events optimized at internal and terminal branches was compared across methods using a paired Wilcoxon rank test.

## RESULTS

### Integrating biogeographical and divergence uncertainty

Figure 4 shows the allcompat consensus of Sapindaceae from MRBAYES with mean values and 95% confidence intervals for nodal ages as estimated by PL analyses over a sample of 1000 trees from the MCMC stationary distribution. Inter-relationships among genera and supra-specific groups were in agreement with Buerki *et al.* (2009), and nearly 95% of all nodes were strongly supported [Bayesian posterior probability (BPP) > 0.95].

Figure 5 depicts cases of soft and hard area incongruence within and between methods (see Fig. 4 and Fig. S1 for the position of nodes on the tree topology). Hard area incongruence cases within LAGRANGE Str are represented in Table 1. Soft area incongruence (i.e. different maximum probabilities assigned to the same ancestral area) was mainly restricted to basal nodes. For example, for nodes 152–153 and 172 corresponding to the first splits within Sapindaceae, all three analyses (Bayes-DIVA, LAGRANGE M1 and Str) recovered area A as the ancestral range but with different relative probabilities (Fig. 6, Fig. S2). Hard area incongruence cases (i.e. different inferred ancestral ranges) were common both at terminal nodes connecting with widespread taxa, for example node 167 (Fig. 6, Fig. S2) leading to *Dodonaea viscosa*, a widespread species distributed in six of the seven defined areas, and at nodes that are shared between two time slices, for example node 294 (Fig. 6, Fig. S2) whose confidence interval spreads across time slices I and II (Figs 4 & 5). The first type of hard area incongruence was more frequent between Bayes-DIVA and the LAGRANGE methods, whereas the second type was more likely to occur between LAGRANGE Str and the two other methods.

Figure 5 shows that biogeographical incongruence was to some extent correlated with dating uncertainty, because the number of soft and hard area incongruent nodes among the three methods was found to increase around the point where there is a transition between time slices. This is particularly true for hard incongruence cases in LAGRANGE Str (Table 1). For example, there is an increase in dating uncertainty at node 154 between TSI and TSII (Figs 4 & 5), which coincides with

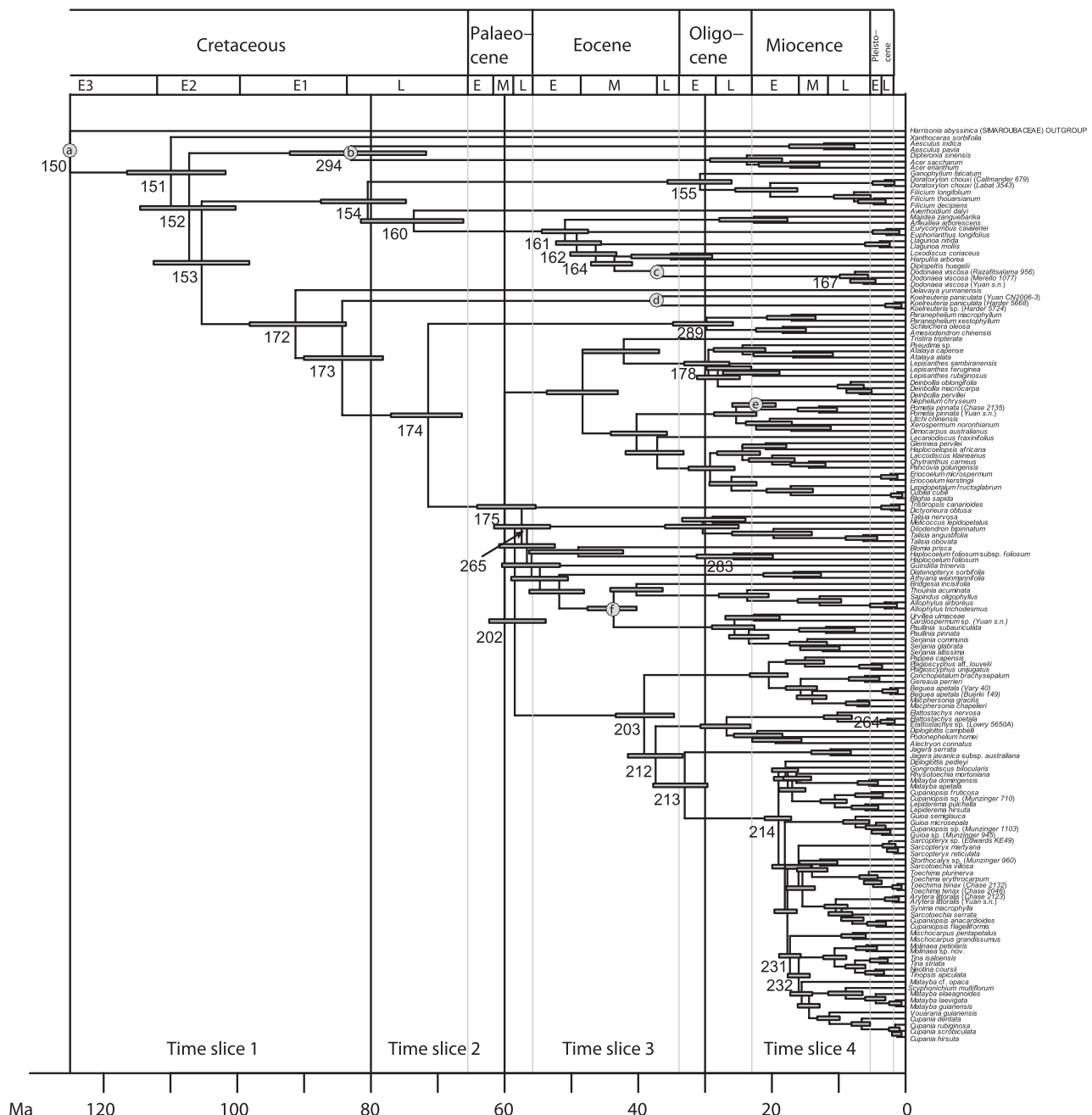


**Figure 4** The median penalized likelihood (Med PL) tree: allcompat consensus tree from the Markov chain Monte Carlo (MCMC) stationary distribution of the Bayesian phylogenetic analysis of Sapindaceae, with median values and 95% confidence intervals for nodal ages as estimated by penalized likelihood over a sample of 1000 stationary trees (see Materials and Methods for an explanation). Numbers refer to nodes that are discussed in the text. Circles 'a' to 'f' represent calibration points used in the dating analyses. Solid lines represent the boundaries between the four time-slices used in the biogeographical analysis (see Fig. 3 for more details); grey lines indicate boundaries for main geological periods.

an increase in biogeographical uncertainty – both in the area assigned (hard incongruence) and in its level of support (soft incongruence) – among the three methods for this node and neighbouring nodes 294, 160 and 174 (Fig. 5). The same pattern can be found for node 155 and neighbouring nodes 289–178 between TSIII and IV and for node 175 and neighbouring nodes 265 and 202 between TSII and III

(Fig. 5, Table 1). This pattern is also found within time slices: for example, for nodes 161–164 within TSIII (Fig. 5). Interestingly, the largest number of hard area incongruent nodes associated to dating uncertainty in LAGRANGE Str was found between TSII and III (Fig. 5), corresponding to a dramatic change in continental configuration between the Laurasian and Gondwanan landmasses (see Fig. 3b,c).

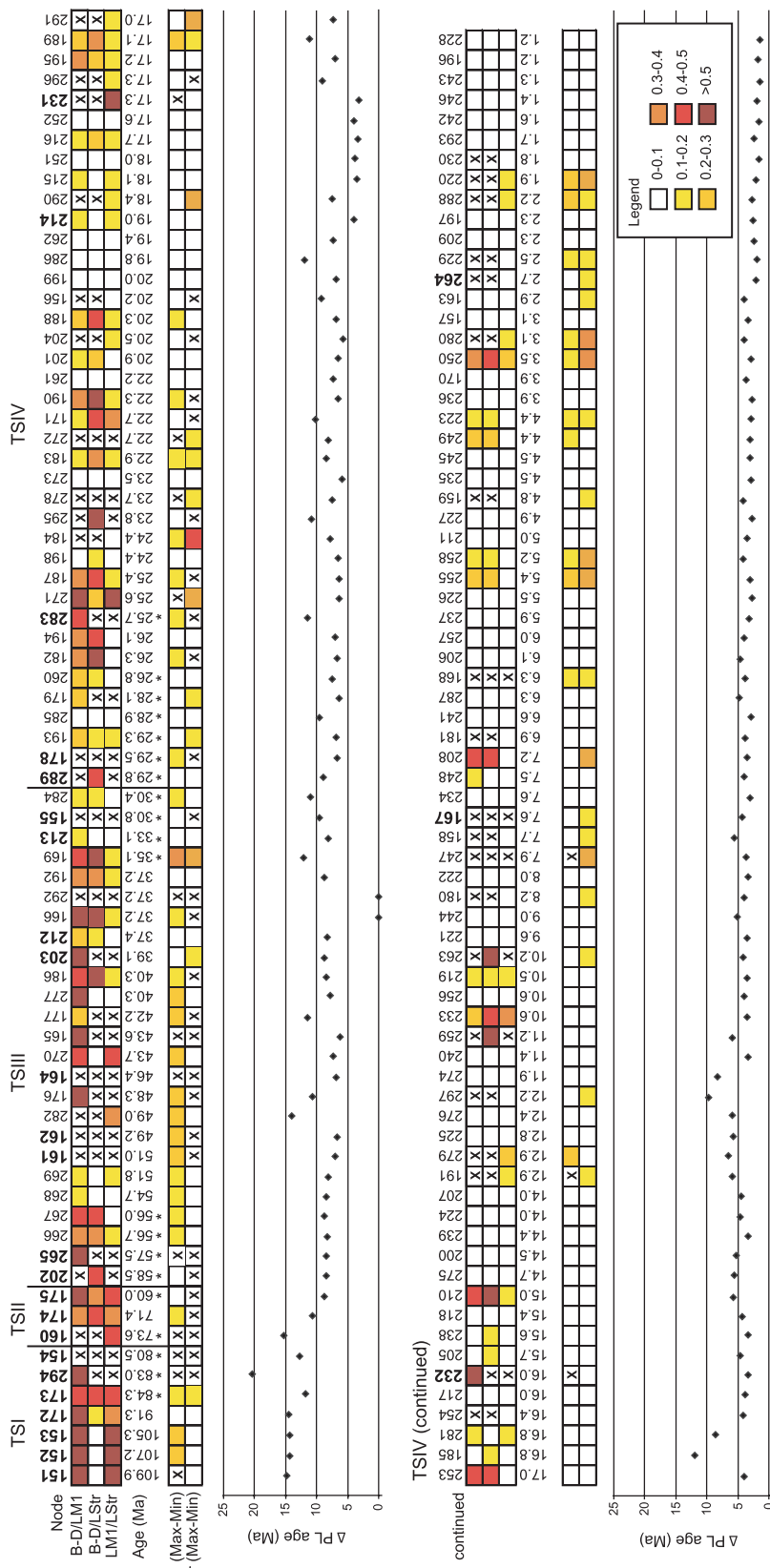


**Figure 5** Effect of divergence-time uncertainty in the biogeographical reconstruction of Sapindaceae. Nodes in the median penalized likelihood (Med PL) tree (see Fig. 4), represented by squares, are sorted according to their age in each time slice. The first three rows represent cases of 'hard' and 'soft' area incongruence in the inference of ancestral ranges – different inferred ancestral ranges – are represented by 'X'. Soft area methods: Bayes-DIVA (B-D) versus LAGRANGE Str (LM1) versus LAGRANGE Str (LM2). Hard area incongruent nodes – are represented by 'X'. Nodes that are shared between maximum probability assigned to the inferred incongruent nodes – the same ancestral range but with different maximum probability – are sorted into six classes according to the difference in maximum probability assigned to the inferred ancestral range (see legend at the bottom). The last two rows represent hard and soft incongruence cases in LAGRANGE M1 and LAGRANGE Str between maximum (Max) and minimum (Min) nodal age estimates (see text for more details). ΔPL represents the uncertainty in divergence-time estimation, measured as the difference between the minimum and maximum nodal age estimates across the sample of 1000 PL-dated trees. The bold lines depict the boundaries of time slices. Nodes that are shared between time slices, and where there is an increase in ΔPL, are marked by '\*'.

**Table 1** Examples of hard area incongruence in nodes shared between two time slices in the LAGRANGE Str reconstruction of Sapindaceae. This is due to dating uncertainty, i.e. differences in the maximum (Max), median (Med) and minimum (Min) nodal ages estimated by penalized likelihood (PL) across a sample of 1000 stationary trees (see Fig. 5 for more details and Fig. 4 for the location of nodes). The ancestral range with the maximum relative probability is indicated for each analysis.

Node	Med age (Ma)	$\Delta$ PL (Ma)	Time slices	LAGRANGE Str		
				Max	Med	Min
294	83	20.4	1–2	A (0.54)	AF (0.49)	AF (0.51)
154	80.48	12.74	1–2	A (0.72)	A (0.72)	AD (0.62)
160	73.59	15.34	1–2	A (0.54)	A (0.42)	AD (0.38)
175	60.02	8.75	2–3	AF (0.36)	D (0.65)	DE (0.56)
202	58.48	8.48	2–3	FG (0.25)	DE (0.67)	E (0.44)
265	57.45	8.4	2–3	G (0.44)	EG (0.59)	EG (0.68)
155	30.75	9.6	3–4	CD (0.22)	D (0.20)	D (0.33)
178	29.5	6.73	3–4	BCD (0.47)	B (0.32)	BD (0.27)
283	25.71	11.43	3–4	G (0.68)	BG (0.57)	BG (0.63)

$\Delta$ PL, difference between the maximum and minimum nodal ages as inferred by PL.

Figure 7 shows pairwise comparison of number of events among the three methods. Bayes-DIVA showed significantly higher maximum probabilities assigned to ancestral area(s) per node than any of the two LAGRANGE methods (Wilcoxon rank test:  $W = 18,189$ ;  $P < 10^{-4}$ ; Fig. 7a). Maximum relative probabilities assigned to ancestral ranges were also higher in LAGRANGE Str than in LAGRANGE M1 but the difference was not significant ( $W = 9639$ ;  $P = 0.110$ ; Fig. 7a). Also, Bayes-DIVA showed a significantly higher number of inferred dispersal events at terminal branches than at internal branches (Wilcoxon rank test:  $W = 9078$ ;  $P = 0.01$ ; Fig. 7b), whereas LAGRANGE M1 and Str showed no significant difference between these two types of dispersal events ( $P$  values of 0.507 and 0.413, respectively; Fig. 7b). On the other hand, global maximum likelihood estimates of dispersal and extinction rates in the Med PL chronogram were 30 times higher in LAGRANGE Str ( $d = 0.025$ ) than in LAGRANGE M1 ( $d = 0.009$ ). Extinction rates were also slightly higher in LAGRANGE Str ( $e = 0.008$ ) than in LAGRANGE M1 ( $e = 0.006$ ).

### Biogeographical scenarios

Figure 6 depicts pairwise comparisons between biogeographical scenarios – ancestral ranges and biogeographical events –

inferred by Bayes-DIVA and LAGRANGE Str. The LAGRANGE M1 biogeographical scenario is presented in Fig. S2.

All three methods agree on inferring that Sapindaceae originated in Eurasia (A) around the Early Cretaceous (TSI; Fig. 6, Fig. S2), with subsequent dispersal to Southeast Asia (D) in the Late Cretaceous or Early Palaeocene (TSI in Bayes-DIVA, TSII in LAGRANGE; Fig. 6, Fig. S2). From there, Sapindaceae ancestors dispersed to Australia–Antarctica (TSII in Bayes-DIVA, TSIII in LAGRANGE), followed by a series of world-wide dispersal events involving both Northern and Southern Hemisphere landmasses (TSIV; Fig. 6, Fig. S2). All three biogeographical scenarios suggest that the Southeast Asian region has been a centre of diversification and dispersal over the tropics for Sapindaceae (Fig. 6, Fig. S2). This is particularly true during TSIV (from the Early Oligocene to the present) with dispersals from Southeast Asia to Australia (E), Africa (B) and Madagascar (C), among others. Reverse migrations are also observed in our biogeographical reconstruction, with several dispersal events from Africa (B) and Australia (E) to Southeast Asia (D), and even from Eurasia (A; most likely Indochina) to Southeast Asia, sometime in the Late Oligocene (Fig. 6, Fig. S2). South American lineages of Sapindaceae probably originated from Australian ancestors, with at least three dispersal events inferred during the Palaeogene (probably through Antarctica; Fig. 3c) and the Miocene (probably mediated by the West Wind Drift current; Fig. 3d). LAGRANGE inferred exchanges between South America and Africa during the last time slice (TSIV; Fig. 6b, Fig. S2) could have been triggered by the South Equatorial Current, which started around this period (Fig. 3d).

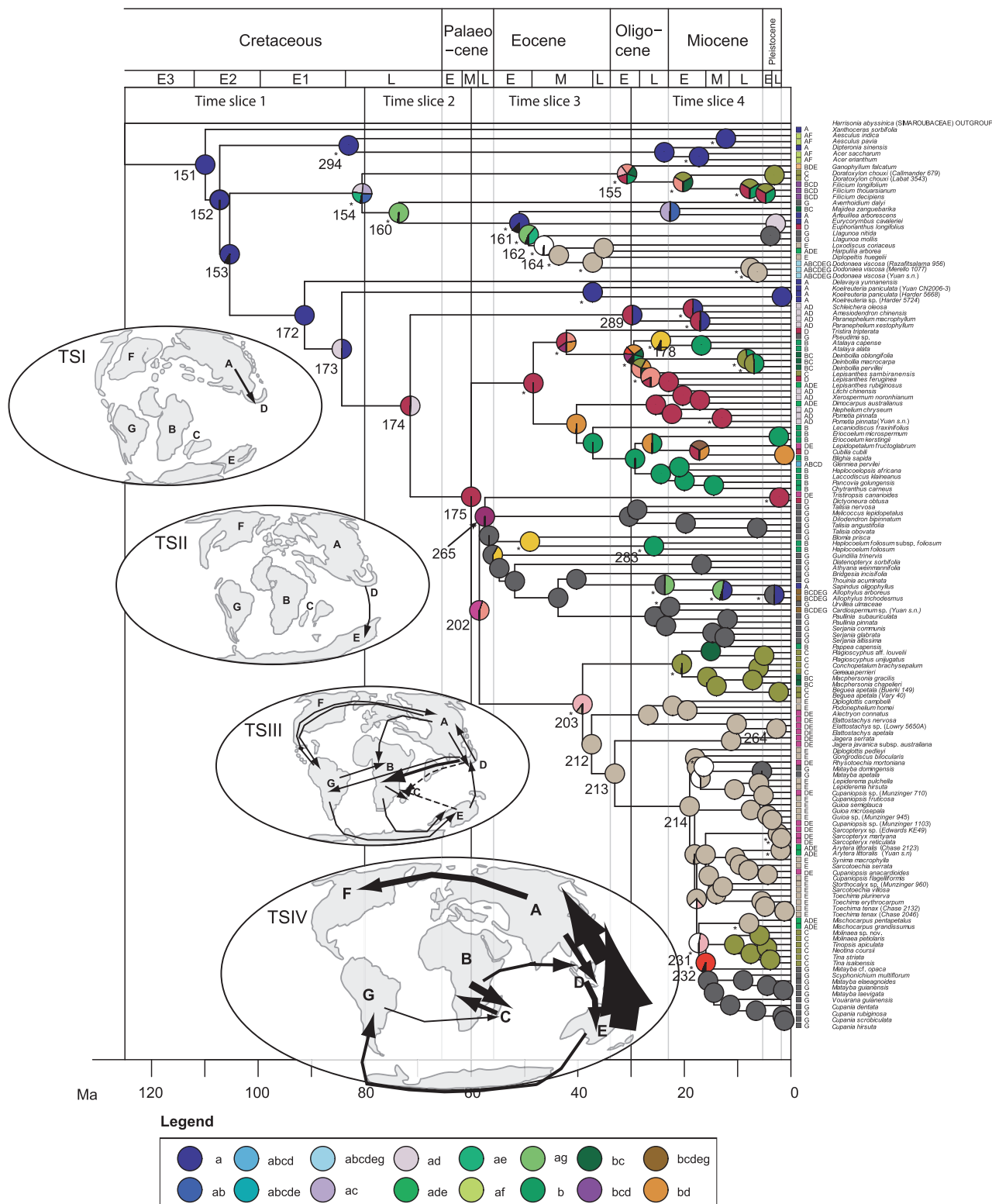
Despite the aforementioned similarities between biogeographical scenarios, the three methods differed in the frequency and timing of biogeographical events. Bayes-DIVA, for example, inferred more dispersal events (70) than LAGRANGE M1 (41) and LAGRANGE Str (57; see also Table S4 in Appendix S2). The highest difference is observed within TSIII, with 13 dispersal events in Bayes-DIVA and only three and seven in LAGRANGE M1 and LAGRANGE Str, respectively (Table S4 in Appendix S2). Another aspect, noticed above, is the observed delay in the timing of dispersal events (biogeographical movements) between Bayes-DIVA and LAGRANGE Str. For example, the dispersal event from Eurasia to proto-Southeast Asia (A to D) early in the history of Sapindaceae is inferred by Bayes-DIVA (Fig. 6a) to have already taken place in TSI (Early Cretaceous, Fig. 3a) but it is pushed forward into TSII (Palaeocene) in the LAGRANGE Str analysis (Fig. 6b). Similarly, the dispersal event from proto-Southeast Asia

**Figure 6** Biogeographical scenarios for Sapindaceae inferred by (a) Bayes-DIVA and (b) LAGRANGE Str plotted onto the median penalized likelihood (Med PL) tree (see Fig. 4). Pie charts represent marginal probabilities (Bayes-DIVA) and relative probabilities (LAGRANGE Str) of ancestral ranges. Biogeographical scenarios are also depicted as frequencies of dispersal events between areas on palaeogeographical maps according to time slices (see Table S4 in Appendix S2 for more details). Solid lines represent the boundaries between the four time slices (see Fig. 3); grey lines indicate boundaries for the main geological periods. Key and abbreviations: junk (black sections of pie charts): sum of ancestral area probabilities  $< 0.1$ ; \*hard area incongruent node between methods; @, hard area incongruent node between the minimum and maximum nodal age estimates (see Fig. 5); TS, time slice. Numbers are provided for those nodes discussed in the text.

to Australia occurs within TSII (Palaeocene) in Bayes-DIVA but it is delayed until TSIII (Mid Tertiary) in LAGRANGE Str.

As expected from a method that does not take time into account, Bayes-DIVA reconstructed 'impossible' dispersal events that did not conform to palaeogeographical history.

a) Bayes-DIVA



One example is the dispersal event from A to D in TSI (Fig. 6; Table S4 in Appendix S2) – area D did not exist at this time (Fig. 3a) – followed by a second dispersal event from D to E in

TSII (these two areas were separated by an ocean gulf during this period; Fig. 3b). Other incongruent dispersal events were the geographical movement from Eurasia (A) to South

b) Lagrange Str

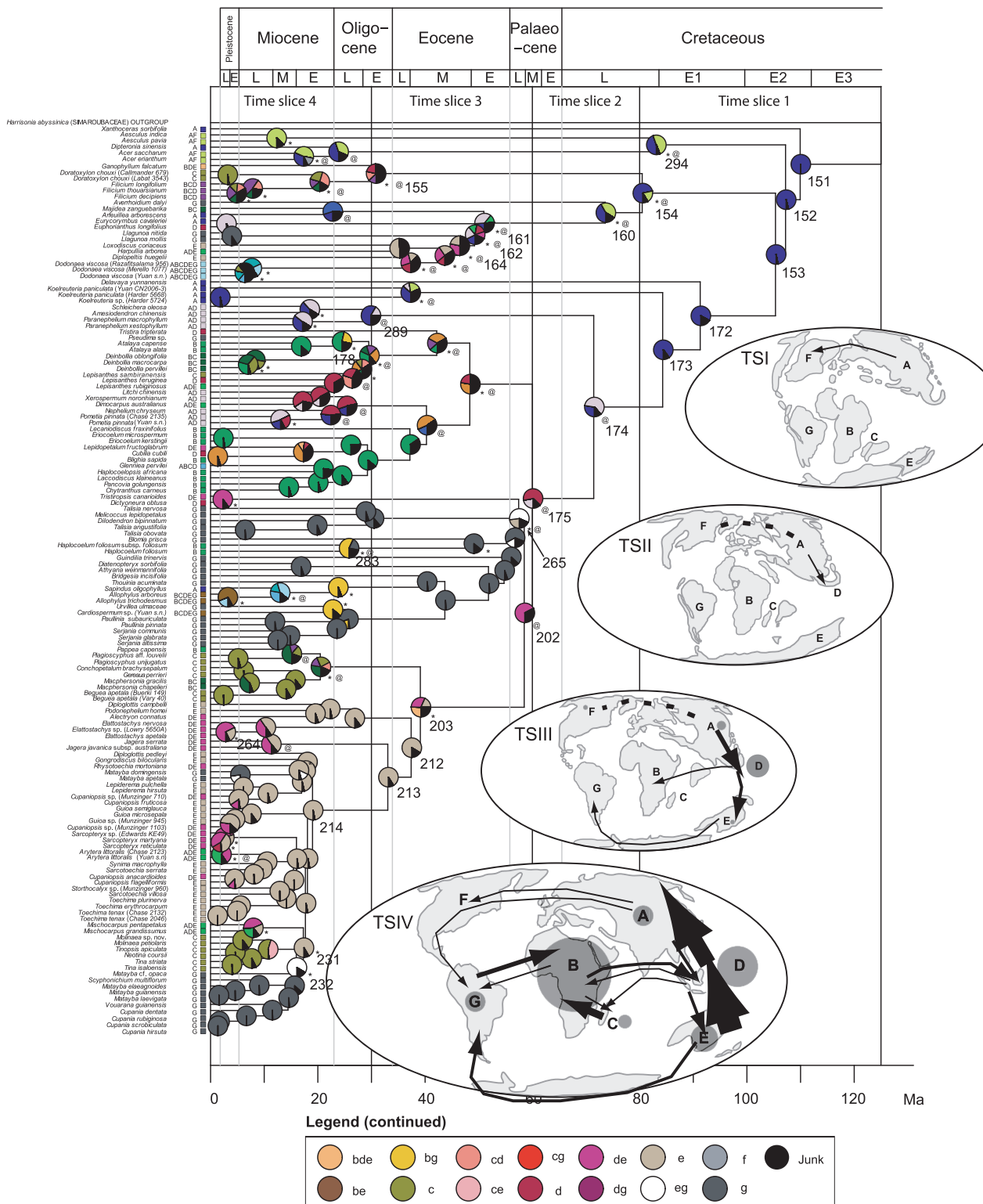
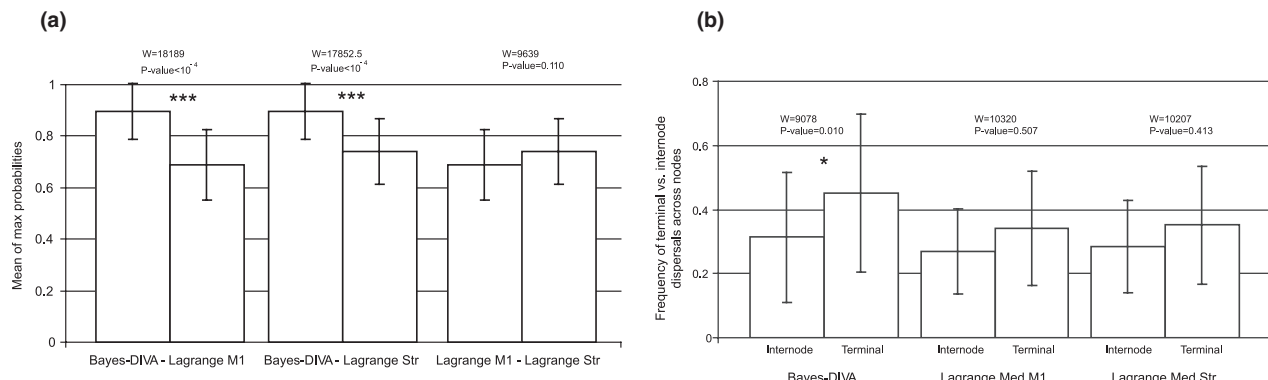


Figure 6 Continued



**Figure 7** Box-whisker plots showing pairwise comparisons between Bayes-DIVA, LAGRANGE M1 and LAGRANGE Str reconstructions of Sapindaceae biogeography for: (a) mean value of maximum probabilities assigned to ancestral ranges and (b) frequency of internode (node-to-node) and terminal (node-to-tip) dispersals estimated across all nodes in the median penalized likelihood (Med PL) tree (see Fig. 4). See text for more details.

America (G) in TSIII (no direct connection between these two areas in Fig. 3c), and the dispersal event from G to C in TSIV (Fig. 6a), which is not supported by the palaeogeographical scenario (i.e. there is no direct land connection in Fig. 3d).

Another aspect in the comparison between biogeographical scenarios is the fact that sometimes LAGRANGE Str infers ancestral ranges at a given internal node that are not part of the geographical distribution of any of its descendants. For example, for node 154 (Fig. 4), the most recent common ancestor (MRCA) of the subfamily Dodonaoideae, LAGRANGE Str infers A (0.716) or AF (0.197) as the most likely ancestral ranges (Fig. 6b). The next node (node 160) is inferred as distributed in A or AF with almost equal probability: 0.42/0.34, respectively (Fig. 6b). Yet, no extant taxon in our analysis belonging to this subfamily is distributed in F (North America) and the taxon diverging most basally in this group (*Averrhoidium*) is restricted to South America (G) (Fig. 6b). A similar case is observed within the *Cupania* group (*sensu* Buerki *et al.*, 2009), whose MRCA (node 232; Figs 4 & 6b) is reconstructed by LAGRANGE Str as widespread in Australia and South America (EG), while all extant taxa in our analysis occur in either Madagascar (C) or South America (G).

Although LAGRANGE M1 (Fig. S2) does not incorporate prior information on the changing palaeogeography into the biogeographical model, it does integrate divergence time information through the use of branch lengths. In general, the LAGRANGE M1 biogeographical scenario was more similar to LAGRANGE Str, and therefore more in agreement with the palaeogeographical model, than were the Bayes-DIVA results. The main dispersal events (from A to D and from D to E) are placed within the same time slices as in LAGRANGE Str (see Fig. S2). On the other hand, LAGRANGE M1 does not show the strange behaviour observed in LAGRANGE Str mentioned above. These nodes (nodes 160, 232) show more uncertainty in ancestral state reconstruction than Bayes-DIVA or LAGRANGE Str (Fig. S2).

**Table 2** Frequency of extinction events ( $E$ ) per area sorted into time slices as inferred by LAGRANGE M1 and LAGRANGE Str reconstructions for Sapindaceae. Numbers between brackets indicate, respectively, ‘observed’ and ‘predicted’ extinction events. See Materials and Methods for more details on area and time slice definitions.

Area	LAGRANGE M1			LAGRANGE Str		
	Time slice 3	Time slice 4	$\sum E$	Time slice 3	Time slice 4	$\sum E$
A	1 (1/0)	2 (2/0)	3	2 (1/2)	3 (2/1)	5
B	1 (1/0)	6 (5/1)	7	0	11 (9/2)	11
C	1 (1/0)	6 (6/0)	7	0	2 (2/0)	2
D	2 (2/0)	7 (6/1)	9	4 (4/1)	6 (6/0)	10
E	0 (0/0)	4 (2/2)	4	1 (1/0)	4 (3/1)	5
F	0 (0/0)	1 (1/0)	1	1 (1/0)	0	1
G	0 (0/0)	2 (1/1)	2	0	3 (2/1)	3
Total	5	28	33	8	29	37

Regarding extinction events (Table 2), LAGRANGE M1 and LAGRANGE Str analyses inferred 33 and 37 events, respectively, distributed over TSIII and IV. Among areas, B and D have the highest number of inferred extinction events, whereas area F has only one extinction event inferred by both analyses (Table 2).

## DISCUSSION

### Integrating geographical information in parametric biogeography

Ree & Sanmartín (2009) point out that the definition of operational areas in a biogeographical analysis constitutes a critical step in parametric biogeography – especially for models considering widespread states (LAGRANGE) – because, the size of the  $Q$  transition matrix increases exponentially with the number of areas. Actually, careful area definition is also important for parsimony-based methods (Bayes-DIVA),

because the greater the number of areas the less often these would be represented among taxa in the phylogeny (i.e. each area could be represented only once), increasing the difficulty of extracting general patterns (e.g. dispersal frequencies) from the data. Using geological information to delimit the operational areas, as done in this study, can be helpful when distribution patterns differ among the study groups and the criterion of sympatry – congruent distribution patterns – is not sufficient. In addition, the circumscription of an area may change through time, as different terranes break up and collide, so the geological history of an area must be considered in its definition. For instance, area D (Southeast Asia) has a complex geological history implying different configurations through time, and this needs to be considered for both defining area boundaries (Fig. 1) and establishing their connection to other areas (Fig. 3), as done in this study.

Ree & Sanmartín (2009) also argued that when the number of states increases relative to the number of data (especially in the case of LAGRANGE), it becomes increasingly worthwhile to impose geographical structure on model parameters governing the transitions between those states. Here we have used this approach in the LAGRANGE Str model, in which dispersal rates were scaled based on the availability of area connections through time (Fig. 3). Ree *et al.* (2005) proposed a similar biogeographical–palaeogeographical model for the Northern Hemisphere, which was later used (and extended) by other authors (e.g. Moore & Donoghue, 2007; Smith, 2009), but to our knowledge, this is the first time such a model has been constructed at a world-wide scale. This approach might prove useful for reconstructing biogeographical history in other cosmopolitan plant families, such as Myrtaceae or Araceae. Further, our model could be used to infer general patterns of dispersal and vicariance across different plant families, or to test large-scale biogeographical hypotheses concerning the spatial evolution of angiosperm families.

Constructing such a broad spatial and temporal model implies some potential risks, including the reducibility of the Markov chain in the biogeographical model. A Markov chain is said to be irreducible if it is possible to get to any state from any state in the matrix. Direct transition between two states (A to B) can be disallowed in the Markov chain Q matrix by assigning it a rate of '0'. However, it should still be possible to change between those two states in the model by using other transition pathways, for example by moving through an intermediate state in the Q matrix (e.g. A to B via AB). When constructing a stratified biogeographical model in which some dispersal pathways are disallowed within time slices, there is a high risk of encountering problems with the reducibility of the Markov chains. In the stratified model, range evolution along internodes (branch lengths) within each time slice is determined by the corresponding Q matrix of that particular period (Fig. 3). Where internal branches cross boundaries between time slices, the likelihood for ancestral ranges is conditional on those ranges being a valid outcome of the preceding period (Ree & Smith, 2008). This may introduce problems with the reducibility of the Markov chain Q matrices. For example, in

our stratified model we encountered the problem with branches that crossed TSII and III because this point marks an important change in continental configuration: in TSII (Fig. 3b), Gondwanan landmasses (B, C, E, G) were still connected, but they broke apart and moved northwards to establish new connections with Laurasia in TSIII (e.g. Australia, Africa, Fig. 3c). One solution to this problem is to use a low but positive scaling value of dispersal such as 0.01, as applied here. This solution is also biologically sound because dispersal events between disjunct landmasses, even though rare, might still be possible. This is even more relevant for several plants, which have seeds that can be easily dispersed. Not allowing dispersal between certain areas, i.e. by assigning them a rate of '0', may be correct in the case of volcanic island systems such as Hawaii, in which islands cannot be colonized before their time of emergence (e.g. Ree & Smith, 2008), but it makes less sense for continental scenarios in which the landmasses were always present, albeit with different size and area connectivity through time. The only exception to this rule was area D, for which dispersal to/from any other area was given a rate of '0' in TSI (Fig. 3a), because this area had not yet been accreted at that time.

Another problem encountered when incorporating palaeogeographical connectivity models into biogeographical analysis (LAGRANGE Str) is the inference of ancestral ranges that are not present in the distribution of the descendants but which are supported by the geological connectivity model. This is the case of the MRCA of the Dodonaeoideae (node 154), which is reconstructed as present in area F when none of extant descendants occurs in this area (see Results and Fig. 4). The explanation lies in the matrix of dispersal rates as constrained by the palaeogeographical model (Fig. 3). Node 154 falls within TSI, a period when Eurasia (A) was only connected to North America (F) through direct land links. In other words, moving from A to any other area would have required going through F (Fig. 3a), so LAGRANGE Str infers this area to be part of the ancestral range of node 154 (Fig. 6b). Similarly, for the *Cupania* group (nodes 231–232, Fig. 6b), the palaeogeographical model (TSIV) disallows direct dispersal between South America and Madagascar, whereas it allows dispersal between these two regions and Australia (scaling factor = 0.5) via the West Wind Drift and the subequatorial currents (Fig. 3). This behaviour is not necessarily a pitfall of the method – the group might have existed in these 'predicted' areas at that particular time but we do not have any fossil evidence. We could test this by applying ecological niche modelling methods. For example, using phyo-climate modelling tools, one may reconstruct the ancestral ecological niche and test whether the inferred ancestral range was potentially within the environmental envelope of the group at that time (e.g. Smith & Donoghue, 2010).

### **Impact of divergence time uncertainty on biogeography**

Most biogeographical studies do not incorporate the error (stochastic variance) associated with estimating lineage

divergence times on phylogenies. At most, they represent dating uncertainty as confidence intervals for divergence-time estimates at nodes, and they interpret the results from the biogeographical reconstruction in view of this uncertainty. Smith (2009) extended the parametric DEC approach to account for uncertainty in topology and divergence-time estimations by running LAGRANGE analysis over a posterior distribution of dated trees generated from a Bayesian divergence-time analysis (BEAST). He showed that accounting for the uncertainty in time estimates has an effect on the likelihood of certain biogeographical scenarios such as the probability of crossing across a land bridge (Smith, 2009). We could not follow this approach here because of the complexity of our geological model (seven areas and four time slices) and the size and taxonomic scale of our dataset (150 taxa, family level). However, our more heuristic approach using the median and extreme values of PL-dated trees confirms that uncertainty in divergence-time estimations indeed has an impact on the biogeographical reconstruction itself, both in the assignment of ancestral ranges to nodes (hard area incongruence) and in the ‘decisiveness’ with which an area can be assigned to a node (soft area incongruence) (Figs 5 & 7, Table 1). Our study suggests that biogeographical uncertainty increases at nodes where dating uncertainty is also high, represented here by the difference between maximum and minimum ages ( $\Delta$ PL) (Figs 4 & 5). This uncertainty can be observed in both LAGRANGE M1 and LAGRANGE Str (Fig. 5) but the effect is even more severe in LAGRANGE Str because its biogeographical model is made directly dependent on a temporally stratified palaeogeographical model (Fig. 3). For example, LAGRANGE Str exhibits the largest number of hard area incongruent nodes (Fig. 5, Table 1) and these are located mainly at nodes whose confidence intervals span two different time slices (Fig. 5, Table 1).

### **Bayes-DIVA versus LAGRANGE: a multivariate problem**

Clark *et al.* (2008) recently reviewed different methods of ancestral range reconstruction using island systems as a case-study biogeographical scenario. They showed that by considering branch lengths and/or the timing of events, parametric methods give more accurate, nuanced inferences of ancestral ranges and biogeographical history than parsimony-based approaches, but that the former methods could benefit from adopting a Bayesian strategy to incorporate phylogenetic uncertainty into biogeographical inference. They concluded that future comparison of methods using different biogeographical systems, such as continental scenarios, are needed to further illustrate the comparative performance of parsimony versus parametric methods (Clark *et al.*, 2008). Continental scenarios differ from island systems in that areas are contiguous (i.e. they share an edge), so widespread ancestral ranges – ancestral distributions formed by two or more areas – are valid states in the biogeographical model and dispersal is generally modelled as the equivalent to ‘range expansion’ (the ancestor moves into a new area but also retains

its original distribution) followed by range division (Sanmartín, 2010). Both DIVA and DEC likelihood models are based on this assumption of ‘vicariance-mediated allopatry’, in which dispersal is modelled as occurring along the branches leading to the widespread node, followed by range division by vicariance (DIVA) or by vicariance and/or peripheral isolate speciation (LAGRANGE) (Fig. 2). In these models, dispersal leads to vicariance but it is not directly associated with cladogenesis (Sanmartín, 2007). This contrasts with character evolutionary models, such as Fitch parsimony optimization or the Bayesian approach to island biogeography developed by Sanmartín *et al.* (2008), in which dispersal between single areas is optimized onto the branches subtending from speciation events (Sanmartín, 2007). In these methods, range evolution is modelled as ‘dispersal-mediated allopatry’, that is, areas are isolated by barriers and dispersal is immediately followed by speciation. Therefore, these methods are more appropriate for island systems in which species are not expected to retain their widespread distribution for long after dispersal (Clark *et al.*, 2008; Sanmartín, 2010).

Despite these similarities, the models implemented by LAGRANGE and DIVA differ in two aspects that have an effect on biogeographical scenarios. In DIVA, widespread ancestral ranges are always divided at speciation nodes by vicariance, whereas LAGRANGE is more flexible than DIVA in that peripheral isolate speciation is allowed for range inheritance scenarios (Fig. 2). The effect of this distinction is twofold. First, DIVA reconstructions tend to overestimate the frequency of terminal dispersal events compared with LAGRANGE (Fig. 7b). Enforcing vicariance on widespread ancestors means that it is more parsimonious for DIVA to explain widespread terminal ranges by assuming terminal dispersal events than inheritance of a more reduced ancestral range with several subsequent internal dispersals (Ree *et al.*, 2005; Nylander *et al.*, 2008a). For example, DIVA would model range evolution from A to ABC as sympatric speciation followed by two terminal dispersals (+B, +C), whereas LAGRANGE would model it as a widespread ancestor (AB or AC) followed by one dispersal event (+B or +C). Therefore, allowing range inheritance by peripheral isolate speciation has the effect in LAGRANGE of increasing the uncertainty in ancestral geographical ranges (i.e. there are more alternative scenarios; see Fig. 7a) but it also diminishes the frequency of terminal dispersals (Fig. 7b). Another unexpected consequence of the different treatment of widespread ranges is that dispersal events in LAGRANGE are delayed in time when compared with the same events in DIVA (e.g. dispersal from D to E in Fig. 6, Fig. S2). As LAGRANGE allows widespread ancestral ranges to be maintained through speciation events (peripheral isolate speciation), there is no need to postulate ‘intermediate’ dispersals to explain why two consecutive ancestral nodes have the same widespread range (AB to AB). For example, the widespread area DE is maintained in LAGRANGE M1 and Str from node 264 to the terminals, whereas DIVA inferred the ancestor in area E and subsequent dispersal events to D in terminal branches (Fig. 6, Fig. S2).

The second difference between the DIVA and LAGRANGE models is the inference of extinction events. As mentioned by Ronquist (1996) and discussed by other authors (Ree *et al.*, 2005; Sanmartín, 2007; Nylander *et al.*, 2008a), DIVA would never infer extinction events unless explicit geographical constraints are used to modify the original cost assignment rules ('constrained DIVA'; Ronquist, 1996). This contributes to an increase in the number of terminal dispersal events, because cases where one descendant is widespread and the other has a more restricted distribution would be inferred by secondary (post-speciation) dispersal in the most widespread descendant (Nylander *et al.*, 2008a). LAGRANGE instead could explain this by peripheral isolate speciation (one descendant inherits the whole ancestral range) or by extinction (one descendant goes extinct in one of the areas). In fact, LAGRANGE does explicitly incorporate extinction into the model as a parameter in the Q matrix that produces range contraction, and in this respect it is more realistic than DIVA. However, by forcing dispersal events between single areas to go through a widespread state, e.g. 'jump dispersal' A to G requires range expansion ( $D_{AG}$ ) followed by extinction ( $E_A$ ) (Fig. 2a), LAGRANGE may overestimate the frequency of extinction events (see Table 2). This is especially the case for those areas where there is a high frequency of interchange with other areas, e.g. area D works as a sort of 'dispersal highway' to other areas in TSIV and has the highest frequency of extinction events (Fig. 6b, Table S4 in Appendix S2). These constraints may be realistic in cases of contiguous areas or areas that come together after the disappearance of a barrier but they are less so in the case of areas separated by ocean barriers (e.g. dispersal mediated by the West Wind Drift, Fig. 3d), for which a model of dispersal-mediated allopatry might be more appropriate.

Another difference between the three methods is their level of 'decisiveness', that is, the different degree of biogeographical uncertainty in assigning ancestral ranges to nodes, 'soft area incongruence' (Figs 5 & 7). Bayes-DIVA is the most 'decisive': maximum probabilities assigned to ancestral ranges at nodes were significantly higher than in the LAGRANGE analyses (Fig. 7a). LAGRANGE Str was more 'decisive' than LAGRANGE M1, although the difference was not significant (Fig. 7a). One reason for this is that LAGRANGE M1 is similar to a parsimony-based method like DIVA in that it has a flat prior on dispersal rates: all dispersal pathways are allowed in the Q matrix and this fact translates into more uncertainty in inferring ancestral ranges. By imposing geographical structure to the model, i.e. by assigning lower rates to certain dispersal pathways, LAGRANGE Str results in higher decisiveness and lower uncertainty than LAGRANGE M1. Likewise, by incorporating uncertainty in the tree topology – the only parameter considered by DIVA when inferring ancestral ranges – Bayes-DIVA shows a higher decisiveness (confidence) in ancestral range reconstruction. However, it should be noted that the ancestral range probabilities estimated by LAGRANGE and Bayes-DIVA are not directly comparable. Bayes-DIVA estimates marginal probabilities by integrating biogeographical

reconstructions over the posterior probability distribution of the tree topology parameter. In contrast, relative probabilities in LAGRANGE are fractions of the global likelihood estimated node-by-node by integrating over all possible range inheritance scenarios in the rest of the tree. Furthermore, the higher 'decisiveness' of Bayes-DIVA in assigning an optimal ancestral area to the node (higher maximum probability) could be partly explained by the fact that only those trees containing the node of interest are considered in estimating marginal probabilities (Nylander *et al.*, 2008a).

## CONCLUSIONS AND PERSPECTIVES

This study analyses the benefits and limitations of parametric approaches to historical biogeographical analysis. It also provides for the first time a world-wide biogeographical model that takes into account area connectivity through time (Fig. 3) and can be used to estimate ancestral ranges and range inheritance scenarios in large cosmopolitan families such as Sapindaceae. Future improvements should focus on: (1) integrating biogeographical, phylogenetic and dating inference uncertainty through the use of a fully Bayesian approach in which divergence times, ancestral ranges and phylogenetic relationships are estimated simultaneously in a composite phylogenetic–biogeographical model; (2) relaxing the assumption of equal dispersal and extinction rates across lineages and areas, for example by incorporating a prior probability on area-extinction rates correlated to area size and on lineage-extinction rates correlated to lineage age; (3) accounting for differences in dispersal capabilities among lineages, e.g. for plant species with fleshy fruits north–south dispersal events are more likely than east–west dispersal events due to the latitudinal migration of birds; the opposite is true for anemochorous fruits, for which east–west winds (e.g. the West Wind Drift) are more important; and finally on (4) coupling lineage diversification with biogeographical range evolution models (Ree & Sanmartín, 2009) to test the hypothesis that dispersal into new areas can lead to accelerated diversification (e.g. Moore & Donoghue, 2007).

## ACKNOWLEDGEMENTS

S.B. would like to thank Philippe Kupfer, Nicolas Salamin, Porter P. Lowry II, Martin W. Callmander and Sylvain G. Razafimandimbison for their support and remarks on the early stages of this study. S.B. and I.S. are also grateful to Fredrik Ronquist (Swedish Museum of Natural History, Stockholm, Sweden) for valuable comments regarding biogeographical analyses during F.R.'s stay at the Real Jardín Botánico. We are also grateful to John Clark and an anonymous referee and to the editor, Brett Riddle, for helpful comments that greatly improved our manuscript. Financial support to S.B. was provided by a Swiss National Science Foundation grant (no. PBNEP3-129903) and by the European Community's Programme Structuring the European Research Area under a SYNTHESYS grant to visit the Real Jardín

Botánico (CSIC) in Madrid. I.S. was funded by the Spanish Ministry of Education and Science (CGL2009-13322-C03-01) and a starting grant from the CSIC-I3 (200830I228).

## REFERENCES

- Antonelli, A., Nylander, J.A.A., Persson, C. & Sanmartín, I. (2009) Tracing the impact of the Andean uplift on Neotropical plant evolution: evidence from the coffee family. *Proceedings of the National Academy of Sciences USA*, **106**, 9749–9754.
- Buerki, S., Forest, F., Acevedo-Rodríguez, P., Callmander, M.W., Nylander, J.A.A., Harrington, M., Sanmartín, I., Küpfer, P. & Alvarez, N. (2009) Plastid and nuclear DNA markers reveal intricate relationships at subfamilial and tribal levels in the soapberry family (Sapindaceae). *Molecular Phylogenetics and Evolution*, **51**, 238–258.
- Buerki, S., Lowry, P.P., II, Phillipson, P.B. & Callmander, M.W. (2010a) Molecular phylogenetic and morphological evidence support recognition of *Gereaua*, a new endemic genus of Sapindaceae from Madagascar. *Systematic Botany*, **35**, 172–180.
- Buerki, S., Lowry, P.P., II, Alvarez, N., Razafimandimbison, S.G., Küpfer, P. & Callmander, M.W. (2010b) Phylogeny and circumscription of Sapindaceae revisited: molecular sequence data, morphology and biogeography support recognition of a new family, Xanthocaraceae. *Plant Ecology and Evolution*, **143**, 148–161.
- Clark, J.R., Ree, R.H., Alfaro, M.E., King, M.G., Wagner, W.L. & Roalson, E.H. (2008) A comparative study in ancestral range reconstruction methods: retracing the uncertain histories of insular lineages. *Systematic Biology*, **57**, 693–707.
- Cox, C.B. (2001) The biogeographic regions reconsidered. *Journal of Biogeography*, **28**, 511–523.
- Croizat, L. (1952) *Manual of phytogeography*. Dr W. Junk, The Hague.
- Donoghue, M.J. & Moore, B.R. (2003) Toward an integrative historical biogeography. *Integrative and Comparative Biology*, **43**, 261–270.
- Drummond, A.J. & Rambaut, A. (2007) BEAST: Bayesian evolutionary analysis by sampling trees. *BMC Evolutionary Biology*, **7**, 214.
- Ebach, M.C., Humphries, C.J. & Williams, D.M. (2003) Phylogenetic biogeography deconstructed. *Journal of Biogeography*, **30**, 1285–1296.
- Espíndola, A., Buerki, S., Bedalov, M., Küpfer, P. & Alvarez, N. (2010) New insights into the phylogenetics and biogeography of *Arum* (Araceae): unravelling its evolutionary history. *Botanical Journal of the Linnean Society*, **163**, 14–32.
- Felsenstein, J. (1988) Phylogenies from molecular sequences: inference and reliability. *Annual Review of Genetics*, **22**, 521–565.
- Forest, F., Nänni, I., Chase, M.W., Crane, P.R. & Hawkins, J.A. (2007) Diversification of a large genus in a continental biodiversity hotspot: temporal and spatial origin of *Muraltia* (Polygalaceae) in the Cape of South Africa. *Molecular Phylogenetics and Evolution*, **43**, 60–74.
- Gradstein, F.M. & Ogg, G.O. (2004) Geologic time scale 2004 – why, how, and where next! *Lethaia*, **37**, 175–181.
- Metcalfe, I. (1998) Paleozoic and Mesozoic geological evolution of the SE Asia region: multidisciplinary constraints and implications for biogeography. *Biogeography and geological evolution of SE Asia* (ed. by R. Halle and J.D. Holloway), pp. 25–41. Backhuys Publishers, Leiden.
- Moore, B.R. & Donoghue, M.J. (2007) Correlates of diversification in the plant clade Dipsacales: geographic movement and evolutionary innovations. *The American Naturalist*, **170**, S29–S55.
- Nelson, G.J. & Platnick, N.I. (1981) *Systematics and biogeography: cladistics and vicariance*. Columbia University Press, New York.
- Nylander, J.A.A. (2004) *MrModeltest v.2*. Program distributed by the author. Evolutionary Biology Centre, Uppsala University, Uppsala. Available at: <http://www.abc.se/~nylander>.
- Nylander, J.A.A., Ronquist, F., Huelsenbeck, J.P. & Nieves-Aldrey, J.L. (2004) Bayesian phylogenetic analysis of combined data. *Systematic Biology*, **53**, 47–67.
- Nylander, J.A.A., Olsson, U., Alström, P. & Sanmartín, I. (2008a) Accounting for phylogenetic uncertainty in biogeography: a Bayesian approach to dispersal-vicariance analysis of the thrushes (Aves: *Turdus*). *Systematic Biology*, **57**, 257–268.
- Nylander, J.A.A., Wilgenbusch, J.C., Warren, D.L. & Swofford, D.L. (2008b) AWTY (are we there yet?): a system for graphical exploration of MCMC convergence in Bayesian phylogenetics. *Bioinformatics*, **24**, 581–583.
- Parenti, L. (2006) Common cause and historical biogeography. *Biogeography in a changing world* (ed. by M.C. Ebach and R.S. Tangney), pp. 61–71. CRC Press, Boca Raton, FL.
- R Development Core Team (2009) *R: a language and environment for statistical computing*. Available at: <http://www.R-project.org>.
- Rambaut, A. & Drummond, A.J. (2007) *Tracer v1.4*. Available at: <http://tree.bio.ed.ac.uk/software/>.
- Ree, R.H. & Sanmartín, I. (2009) Prospects and challenges for parametric models in historical biogeographical inference. *Journal of Biogeography*, **36**, 1211–1220.
- Ree, R.H. & Smith, S.A. (2008) Maximum likelihood inference of geographic range evolution by dispersal, local extinction, and cladogenesis. *Systematic Biology*, **57**, 4–14.
- Ree, R.H., Moore, B.R., Webb, C.O. & Donoghue, M.J. (2005) A likelihood framework for inferring the evolution of geographic range on phylogenetic trees. *Evolution*, **59**, 2299–2311.
- Ronquist, F. (1996) *DIVA 1.2*. Computer program distributed by the author. Available at: <http://www.ebc.uu.se/systzoo/research/diva/diva.html>.
- Ronquist, F. (1997) Dispersal-vicariance analysis: a new approach to the quantification of historical biogeography. *Systematic Biology*, **46**, 195–203.

- Ronquist, F. (2003) Parsimony analysis of coevolving associations. *Tangled trees: phylogeny, cospeciation, and coevolution* (ed. by R.D.M. Page), pp. 22–64. University of Chicago Press, Chicago, IL.
- Ronquist, F. & Huelsenbeck, J.P. (2003) MrBayes 3: Bayesian phylogenetic inference under mixed models. *Bioinformatics*, **19**, 1572–1574.
- Roquet, C., Sanmartín, I., García-Jacas, N., Sáez, L., Wikström, N. & Aldasoro, J.J. (2009) Reconstructing the history of Campanulaceae s. str. with a Bayesian approach to molecular dating and dispersal–vicariance analysis. *Molecular Phylogenetics and Evolution*, **52**, 575–587.
- Sanderson, M.J. (2002) Estimating absolute rates of molecular evolution and divergence times: a penalized likelihood approach. *Molecular Biology and Evolution*, **19**, 101–109.
- Sanderson, M.J. (2004) *r8S, program and documentation*. Version 1.7.1. Available at: <http://loco.biosci.arizona.edu/r8s/>.
- Sanmartín, I. (2007) Event-based biogeography: integrating patterns, processes, and time. *Biogeography in a changing world* (ed. by M.C. Ebach and R. Tangney), pp. 135–159. CRC Press, Boca Raton, FL.
- Sanmartín, I. (2010) Breaking the chains of parsimony: parametric mode-based approaches to historical biogeography. *Biogeography: an ecological and evolutionary approach*, 7th edn (ed. by B.C. Cox and P.D. Moore), pp. 213–214. Blackwell Publishing, Oxford.
- Sanmartín, I. & Ronquist, F. (2004) Southern Hemisphere biogeography inferred by event-based models: plant versus animal patterns. *Systematic Biology*, **53**, 1–28.
- Sanmartín, I., Enghoff, H. & Ronquist, F. (2001) Patterns of animal dispersal, vicariance and diversification in the Holarctic. *Biological Journal of the Linnean Society*, **73**, 345–390.
- Sanmartín, I., van der Mark, P. & Ronquist, F. (2008) Inferring dispersal: a Bayesian approach to phylogeny-based island biogeography, with special reference to the Canary Islands. *Journal of Biogeography*, **35**, 428–449.
- Sanmartín, I., Anderson, C.L., Alarcon-Cavero, M.L., Ronquist, F. & Aldasoro, J.J. (2010) Bayesian island biogeography in a continental setting: the Rand Flora case. *Biology Letters*, **6**, 703–707.
- Santos, J.C., Coloma, L.A., Summers, K., Caldwell, K.P., Ree, R. & Cannatella, D.C. (2009) Amazonian amphibian diversity is primarily derived from Late Miocene Andean lineages. *PLoS Biology*, **7**, 448–461.
- Smith, S.A. (2009) Taking into account phylogenetic and divergence-time uncertainty in a parametric biogeographic analysis of the Northern Hemisphere plant clade Caprifolieae. *Journal of Biogeography*, **36**, 2324–2337.
- Smith, S.A. & Donoghue, M.J. (2010) Combining historical biogeography with niche modeling in the *Caprifolium* clade of *Lonicera* (Caprifoliaceae, Dipsacales). *Systematic Biology*, **59**, 322–341.
- Stamatakis, A. (2006) RAxML-VI-HPC: maximum likelihood-based phylogenetic analyses with thousands of taxa and mixed models. *Bioinformatics*, **22**, 2688–2690.
- Xiang, Q.Y.J. & Thomas, D.T. (2008) Tracking character evolution and biogeographic history through time in Cornaceae – does choice of methods matter? *Journal of Systematics and Evolution*, **46**, 349–374.

## SUPPORTING INFORMATION

Additional Supporting Information may be found in the online version of this article:

**Appendix S1** Expanded materials and methods. (a) List of fossils (and associated references) used in the phylogenetic dating analysis. (b) Description of the palaeogeographical model used in the LAGRANGE Str analysis.

**Appendix S2** Supplementary tables. Tables S1–S3: contingency tables showing number and type of biogeographical events inferred by Bayes-DIVA, LAGRANGE M1 and LAGRANGE Str, respectively. Table S4 shows for each method the frequency of dispersal events between areas, sorted by time slices.

**Figure S1** The location of nodes in the Sapindaceae phylogeny.

**Figure S2** The biogeographical scenario – ancestral ranges and biogeographical events – inferred by LAGRANGE M1 analysis.

As a service to our authors and readers, this journal provides supporting information supplied by the authors. Such materials are peer-reviewed and may be re-organized for online delivery, but are not copy-edited or typeset. Technical support issues arising from supporting information (other than missing files) should be addressed to the authors.

## BIOSKETCH

**Sven Buerki** is a post-doctoral fellow at the Real Jardín Botánico of Madrid (Spain), funded by the Swiss National Science Foundation, under the supervision of Professor Isabel Sanmartín. His research is focused on understanding the spatio-temporal evolution of various plant families, e.g. Sapindaceae and Pandanaceae. He is also interested in the development of new methods in the field of biogeography.

Author contributions: S.B. and I.S. conceived the ideas; S.B. collected the data; all authors contributed to the analysis of the data; S.B. and I.S. led the writing.

---

Editor: Brett Riddle